Crustal origin of Hercynian peraluminous granitic batholiths of Central Spain: petrological, geochemical and isotopic (Sr, Nd) constraints

C. Villaseca [a,*], L. Barbero [b,1], G. Rogers [c,2]

[a] *Dpto. Petrología y Geoquímica, Fac. C.C. Geológicas, Universidad Complutense, 28040 Madrid, Spain*
[b] *Dpto. Geología, Fac. C.C. del Mar, Universidad de Cádiz, 11510 Puerto Real, Cádiz, Spain*
[c] *Isotope Geosciences Unit, Scottish Universities Research and Reactor Centre, East Kilbride, Glasgow, G75 0QF, UK*

Abstract

In Central Spain, it is possible to distinguish two main types of peraluminous late-Hercynian granites: the PI types and the PS types. The distinction between both types is made on the basis of differences in peraluminosity (PS types are more peraluminous than PI types) and also on the appearance of some characteristic mafic minerals; PS types have biotite, cordierite and monazite as the most typical accessory phase, whereas PI types have biotite, amphibole (in the less evolved facies) and allanite as the accessory mineral. Both granite types have similar trace element ratios and initial Sr, Nd and Pb isotopic signatures. Initial $^{87}Sr/^{86}Sr$ ratios of both types exhibit a large range from 0.7073 to 0.7193, whereas initial ε_{Nd} varies in a restricted range from -5.4 to -6.6. The scarce associated basic rocks do not play a significant role in the chemical variability of these peraluminous granites which follow low pressure crystal fractionation trends from granodiorite/monzogranite parental magmas. Mixing and AFC modelling of Sr and Nd isotopic data reveal an unrealistically high mantle contribution. Based on major and trace element and isotopic data, an orthogneissic protolith for both granitic series is proposed. Nevertheless, none of the metamorphic country rocks of Central Spain has the appropriate Sr isotopic composition to satisfy the origin of these granitic rocks, and so, it is argued that progressive isotopic re-equilibration of crustal material during the granulization of the lower Hercynian crust, together with the possibility of isotopic disequilibrium during melting (as has been demonstrated in migmatitic terranes in nearby areas) may explain the isotopic differences between the granites and the high level metamorphic country rocks. © 1998 Elsevier Science B.V. All rights reserved.

Keywords: Igneous; Peraluminous granites; Iberian Hercynian Belt; Geochemistry; Sr–Nd isotopes; Central Spain

1. Introduction

Compared with other collisional orogenic belts, the Hercynides are characterised by the emplacement of large volumes of felsic magmas of various compositions. The area of the present study comprises

---

* Corresponding author. Fax: +34-1-5442535; e-mail: granito@eucmax.sim.ucm.es.

[1] Fax: +34-56-470811; e-mail: luis.barbero@uca.es.

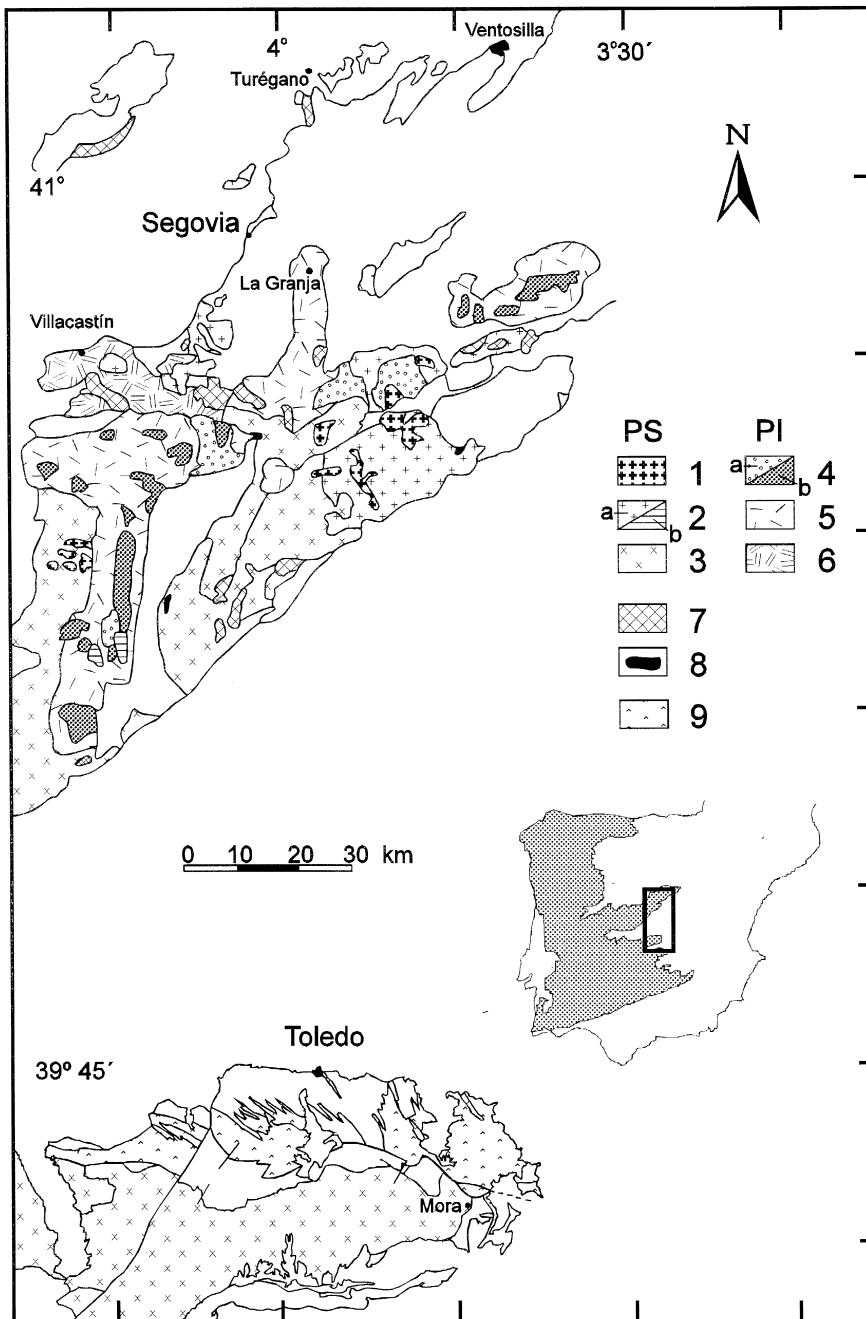[2] E-mail: g.rogers@surrc.gla.ac.uk.

Fig. 1. Geological sketch map with typology of granites in Central Spain: northern branch is Sierra de Guadarrama; southern branch is Montes de Toledo. Legend: PS-types: 1 = Leucogranites, 2a = coarse-grained granites, 2b = fine-grained granites, 3 = granodiorites/monzogranites, PI-types: 4a = coarse-grained leucogranites, 4b = fine-grained leucogranites, 5 = granites, 6 = granodiorites/monzogranites, 7 = unassigned granites, 8 = basic–intermediate rocks, 9 = migmatite terrain granites.

the eastern parts of the Spanish Central System (Sierra de Guadarrama s.l.) and the Montes de Toledo (Fig. 1). This region shows the general characteristics of Hercynian magmatism. First, the plutonic rocks represent a huge proportion of the orogenic area: in the Spanish Central Region (SCR), granitoids comprise more than 70% of the total surface outcrop. Second, the proportions of gabbro–diorite:tonalite–granodiorite:granite are 1:11:88 with the granitic rocks being dominantly felsic and almost exclusively of peraluminous composition. These proportions contrast markedly with those found both in continental margins (gabbro–diorite: tonalite–granodiorite: and granite are 16:58:26; Pitcher, 1978), and in other ensialic orogens (Himalayan areas with 0:0:100, Le Fort et al., 1987), suggesting that different sources and/or different melting or crystallization processes were involved in granite petrogenesis.

The late-Hercynian plutonism of the SCR has been studied in detail during the last 10 years (e.g., Brandebourger, 1984; Casillas, 1989; Andonaegui, 1990; Pérez-Soba, 1991; Villaseca et al., 1993; Villaseca and Barbero, 1994a) with two main granite types being distinguished. The first is composed of cordierite-bearing granites, hereafter called PS types, which are generally strongly peraluminous (A/CNK values between 1.05–1.20). The second type is composed of metaluminous to moderately peraluminous granites (A/CNK in the range 0.95–1.10), (hereafter termed PI types) characterised by the occurrence of biotite as the dominant mafic phase, with scarce amphibole in the marginal granodioritic facies, and rare accessory garnet (or exceptionally cordierite) in the most fractionated leucogranites (Villaseca and Barbero, 1994a). Scarce basic and intermediate rocks are spatially associated with both granite types; although according to their major and trace element chemistry (Casillas, 1989), they do not seem to contribute to the chemical variability of the peraluminous granites.

Most of these granitic magmas have been ascribed to melting of the continental crust due to crustal thickening after the main Hercynian continental collision (Brandebourger, 1984; Casillas, 1989). The aim of this paper is to provide better constraints on genetic models for the generation of granites of the SCR, the most intracontinental region of the Iberian Hercynian Belt.

2. Geological framework

The oldest rocks in this part of the SCR mainly comprise meta-sedimentary pelitic schists which are Proterozoic and Lower Palaeozoic in age, and meta-igneous rocks (augen gneisses) of Cambro-Ordovician age (500 ± 20 Ma, Vialette et al., 1987; Valverde-Vaquero et al., 1995). Discordant U–Pb zircon data from both meta-sedimentary and meta-igneous rocks of the SCR give lower concordia intercepts around 370–380 Ma (Wildberg et al., 1989) that are considered to mark the beginning of the Hercynian crustal thickening. The subsequent high pressure–high temperature metamorphic event is recorded in scarce eclogitic and high P-granulite facies rocks (Villaseca and Barbero, 1994b). This was followed by higher T, lower P evolution dated at 335 Ma ± 5 Ma by U–Pb in monazites from metasediments and meta-igneous rocks from the Sierra de Guadarrama (Valverde-Vaquero et al., 1995). During the Hercynian metamorphic climax, wide zones of the middle crust in the Sierra de Guadarrama and Montes de Toledo underwent partial melting (Barbero, 1995). The late-Hercynian evolution (325–280 Ma) was dominated by extensional tectonics and pervasive retrograde metamorphism of the middle and upper Hercynian crust. Listric and transcurrent faults played a crucial role in the emplacement of major granite batholiths at this time (Doblas, 1991). The studied part of the SCR contains two different batholithic segments: the eastern part of the Sierra de Guadarrama, and, to the south, the Mora–Las Ventas batholith (Fig. 1). The different plutons which comprise both segments intrude both meta-sedimentary and metaigneous rocks. The main groups of granitoids which comprise the large massifs of the area were formed after the peak of metamorphism, and are the main objective of this work. These granites generate typical contact aureoles in the surrounding wall-rocks, indicating their allochthonous character and high emplacement level (5–8-km depth). The partial melting which produced the late granitic batholiths must have occurred at deeper crustal levels than those represented by the exhumed middle-crustal granulite facies terranes, into which they finally intrude.

This late-Hercynian granitic magmatism occurred between 50 and 60 Ma after the beginning of the

continental collision, and post-dated the main tectono-metamorphic events. Such diachronism is expected with partial melting processes originating at lower crustal levels in tectonic thickening models (England and Thompson, 1986). There is no spatial or temporal distribution of the PS and PI types in the area. Between 330 to 280 Ma, an enormous (more than 15,000 km^2) batholith with more than a hundred intrusions was formed in the Spanish Central Region (Fig. 1). Although there appears to have been continuous magmatism during this period, it seems that there were at least two main pulses of magmatic activity, the first one around 320 ± 5 Ma and the second around 295 ± 10 Ma (Villaseca et al., 1995). The first pulse corresponds to the intrusion of large plutonic complexes along major crustal detachments, whereas in the second, the number of plutons increases but their volume decreases.

3. Petrological characterization

The basic and intermediate rocks are of limited occurrence and appear as small plutons and unconnected masses usually with outcrops of less than 2 km^2 (Table 1). They appear either as small plutons with contact aureoles in metamorphic areas (Villaseca et al., 1993), or as variably brecciated bodies within the penecontemporaneous granitic intrusions (Casillas, 1989). One of these basic massif has been dated by Rb–Sr whole-rock methods at 322 ± 5 Ma (Casillas et al., 1991), which coincides with the age of the first pulse of granite plutonism (Table 1).

Petrographically, there are two main types: quartz–diorites with isolated gabbroic–dioritic facies (El Tiemblo), and essentially tonalitic–granodioritic masses such as Ventosilla (Casillas, 1989). These rocks have variable modal proportions of quartz,

Table 1
Central Spain pluton features

Pluton	Area (Km^2)	Shape	Facies	Rock types	Age (Ma)	$(^{87}Sr/^{86}Sr)_i *$	$(\varepsilon_{Nd})_i$
Basic–intermediate rocks (BIR)							
El Tiemblo	1	elongate	cm	gb, dt, qdt, ton (fol)	322 ± 5[a]	0.70765	-4.64[a]
Ventosilla	2	circular	cm	ton, gdt	?	0.70888	-5.85
PI types							
Villacastín	150	irregular	cm	hbl–bt gdt, bt mzgr	323 ± 47[b]	0.7073	-5.53
La Cabrera	160	kidney	cm	hbl–bt gdt, bt mzgr, bt lgr	310 ± 14[c]	0.7094	-6.53
Navas del Marqués	300	irr. elong.	cm	hbl–bt gdt, bt (mzgr, lgr)	302 ± 4[a]	?	?
La Pedriza	75	circular	sf	bt lgr	307 ± 3[d]	0.70797	?
La Granja	85?	elongate	cm	hbl–bt gdt, bt mzgr	299 ± 55[b]	0.71212	-6.49
Atalaya Real	18	circular	cm	hbl–bt (gdt, mzgr, lgr)	284 ± 13[b]	0.7129	-6.00
PS types							
Mora–Las Ventas	515	elongate	cm	bt ± cdt (gdt, mzgr, lgr)	320 ± 8[e]	0.7103	-6.37
Alpedrete	350	irregular	cm	bt ± cdt (gdt, mzgr, lgr)	?	0.70896	-6.31
Hoyo de Pinares	130?	irr. elong.	cm	bt gdt, bt ± cdt (mzgr, lgr)	301 ± 15[a]	?	?
Cebreros	150?	irr. elong.	cm	bt gdt, (mzgr, lgr)	320 ± 11[a]	?	?
Cardín	225	irregular	cm	bt ± cdt (mzgr, lgr)	?	0.71369	-6.25
Cabeza Mediana	7	circular	sf	bt ± cdt lgr	291 ± 6[d]	0.71127	-6.64
El Berrocal	15	circular	sf	bt–ms lgr	290 ± 1[f]	0.72540	?

Abbreviations: cm, composite pluton; sf, single facies; gb, gabbro; dt, diorite; qdt, quartz–diorite; ton, tonalite; fol, foliated; gdt, granodiorite; mzgr, monzogranite; lgr, leucogranite; hbl, hornblende; bt, biotite; cdt, cordierite; ms, muscovite.
$(^{87}Sr/^{86}Sr)_i *$ calculated at 300 Ma when no isochron is available (Ventosilla, Alpedrete, Cardín). Error on ages are $\pm 2\sigma$, but for isochrons of Villacastín and La Granja, the age errors were multiplied by $(MSWD)^{1/2}$ when MSWD exceeded 1 (enhanced error method after Williamson, 1968), increasing by a factor between 3–6 times the age error (Villaseca et al., 1995).
References: [a]Casillas et al. (1991), [b]Villaseca et al. (1995), [c]Vialette et al. (1981), [d]Ibarrola et al. (1987), [e]Andonaegui (1990), [f]Lallena et al. (1990).

potash feldspar and zoned plagioclase with highly calcic cores (up to An_{85}). The main ferromagnesian phases are biotite, amphibole and pyroxene. Accessory phases include apatite, zircon, allanite and ilmenite.

PI and PS granitic types comprise batholiths (plutonic complexes over 100 km^2) of a composite character, in several of which it is possible to distinguish over a dozen individual intrusive units. The compositional variation found in these major plutons usually ranges from granodiorites to leucogranites. However, tonalitic and more basic rocks are included as large xenoliths in some of these plutons, although their total volume is insignificant. A very common feature of both granitic types is the conspicuous presence of mafic microgranular enclaves dispersed in the plutons, especially in the granodiorites and monzogranites. This is undoubtedly the most abundant enclave type.

Differences between the PI and PS intrusions are evident especially when considering the igneous mineral paragenesis. The typical AFM mineral assemblages in the PS granites are: biotite and cordierite in granodiorites–monzogranites and biotite, cordierite $\pm$ alumino silicates in leucogranites, always with apatite, zircon, monazite, xenotime and ilmenite as the most frequent accessories. In the PI granites, the main AFM phases are: biotite with rare amphibole in granodiorites–monzogranites, and biotite $\pm$ garnet in leucogranites, with apatite, zircon, allanite, titanite, monazite, xenotime and ilmenite–magnetite as accessory phases. However, some mineral convergence occurs in the highly fractionated leucogranites of both magmatic series. For example, garnet can also appear in the more acid PS types and cordierite may also be present in the very acid PI types (La Cabrera nodular leucogranites, Villaseca and Barbero, 1994a). In some granodioritic–monzogranitic PI facies, amphibole occurs sporadically, and clinopyroxene even more rarely. The latter usually shows residual textures, included in first generation plagioclase or poikilitically enclosed by amphibole. Its composition varies between augite and diopside without substantial change in the Fe/Mg ratio. Euhedral amphibole is enclosed by plagioclase and is considered to be magmatic, whereas other amphibole crystals are clearly ex-

solved and recrystallized as subsolidus actinolite. The igneous amphiboles vary in composition from titanian ferro-edenites (with $(Na + K)_A \geq 0.5$) to Mg-hornblendes. A detailed study of the chemical variability of AFM minerals in both granitic series can be found in Villaseca and Barbero (1994a).

4. Analytical techniques

Between 8 and 15 kg of fresh rock sample were collected for chemical analysis. Major and trace elements were measured at Universidad Complutense de Madrid (Spain). Samples were dissolved using a mixture of HF and $HClO_3$ in platinum crucibles. Major elements were determined by ICP-AES techniques using a Jovin–Yvon 38 plus spectrometer. FeO was determined by titration. Trace elements were measured by XRF in a Phillips PW1510 spectrometer. Around half of the samples were duplicated for major and trace elements by ICP-AES at CNRS (Nancy) giving consistent results. In these analyses, all iron is given as Fe_2O_3 (see Table 2). Rare earth elements were measured by ICP-MS at CNRS (Nancy, France) following the method of Govindaraju and Mevelle (1987). Representative chemical analyses of SCR granites are given in Table 2.

Isotopic determinations for Sr and Nd were performed at the Scottish Universities Research and Reactor Centre, using techniques described in Barbero et al. (1995). Sr samples were run on a VG 54 E thermal ionisation mass spectrometer. The $^{87}Sr / ^{86}Sr$ ratio was corrected for mass fractionation using $^{86}Sr / ^{88}Sr = 0.1194$. Repeat analysis of NBS 987 Sr standard gave $^{87}Sr / ^{86}Sr = 0.71023 \pm 4$ (2 s.d., $n = 30$). Nd isotope ratio analyses were performed on a VG Sector 54–30 thermal ionisation mass spectrometer with data acquired in multi-dynamic mode. $^{143}Nd / ^{144}Nd$ ratios were corrected for mass fractionation using $^{146}Nd / ^{144}Nd = 0.7219$. During the course of this study, the Johnson and Matthey Nd standard gave $^{143}Nd / ^{144}Nd = 0.511500 \pm 10$ (2 s.d., $n = 35$). Sm and Nd isotope dilution analyses were performed on the same mass spectrometer in static mode. Measured Sm/Nd ratios are

Table 2

Representative chemical analyses of basic and intermediate rocks (BIR), and PI and PS granites from Central Spain

| | BIR | | | | PI granites | | | | | | | | | | |
| | El Tiemblo | | Ventosilla | | Atalaya Real | | | | | La Cabrera | | | | | |
	83535	83534	60121	60864	95922	96026	96029	96024	96022	55718	55763	56205	55766	55702	56201
SiO_2	52.13	58.43	60.50	62.00	67.28	69.23	71.49	74.80	76.48	65.95	66.34	69.09	69.65	75.68	77.06
TiO_2	0.61	1.06	0.89	0.83	0.44	0.34	0.21	0.09	0.03	0.50	0.56	0.40	0.38	0.06	0.02
Al_2O_3	18.22	16.91	15.88	16.39	15.89	14.80	14.47	12.80	12.34	15.73	15.58	14.96	14.63	12.73	12.60
FeO_3	0.79	0.93	1.19	1.38	0.55	0.48	0.34	0.24	0.16	4.29	4.47	3.22	3.45	1.41	0.96
FeO	5.64	5.46	4.69	4.05	3.09	2.67	1.89	1.38	0.92						
MnO	0.12	0.12	0.09	0.07	0.04	0.04	0.02	0.03	0.01	0.06	0.06	0.04	0.05	0.03	0.06
MgO	8.29	3.62	3.63	2.87	0.87	0.68	0.38	0.18	0.07	1.35	1.38	0.81	0.81	0.12	0.03
CaO	8.56	6.22	5.89	5.89	3.34	2.58	2.11	1.01	0.83	3.40	3.41	2.79	2.37	0.96	0.39
Na_2O	2.15	3.04	3.02	3.07	3.27	3.22	3.22	3.32	3.53	3.39	3.25	3.20	3.24	3.17	3.41
K_2O	0.98	2.43	2.36	2.31	4.16	4.46	5.04	4.92	4.57	3.59	3.65	4.00	4.25	4.65	4.48
P_2O_5	0.12	0.34	0.24	0.20	0.16	0.14	0.08	0.04	0.02	0.14	0.16	0.13	0.12	0.02	0.01
LOI	1.61	0.99	1.59	0.94	0.70	1.16	0.54	1.06	0.94	1.36	0.87	1.12	0.82	0.99	0.82
TOTAL	99.22	99.55	99.53	99.96	99.79	99.80	99.79	99.87	99.90	99.76	99.73	99.76	99.77	99.82	99.83
A/CNK	0.90	0.89	0.87	0.90	1.00	1.00	0.99	1.01	1.01	1.01	1.01	1.02	1.03	1.06	1.13
Ba	241	539	667	681	777	579	631	209	37	598	605	624	554	108	19
Rb	39	85	75	81	172	190	199	270	240	145	138	141	165	223	308
Sr	172	160	362	364	167	132	111	35	12	193	192	162	132	41	10
Y	17	22	26	25	27	32	33	43	28	27	27	27	30	45	60
Zr	85	99	136	143	213	180	125	106	49	140	150	151	153	61	48
Nb	11	18			11	11	8	11	9	2	2	3	3	3	2
Th	2	8	15	12	15	17	15	19	18	14	9	17	20	22	18
U															
V					37	29	18	7	2	47	48	30	29	3	2
Cr	542	241	31	16	58	91	156	122	72	22	24	13	13	3	3
Ni	39	17	6	7	6	7	8	6	4	9	9	2	8	2	2
La	12.12	23.44	27.87	28.80	50.73	31.39	27.46	24.30	12.74	43.07	34.13	43.36	39.07	17.26	13.25
Ce	28.97	50.88	56.40	61.73	103.50	67.45	59.78	54.23	29.54	94.38	64.39	85.73	85.20	40.29	34.56
Nd	12.09	20.20	25.09	25.97	44.04	30.43	28.02	25.53	15.45	39.85	27.86	35.91	35.81	20.86	19.64
Sm	3.04	4.70	5.47	5.56	7.98	6.83	6.55	6.48	4.37	5.85	4.58	7.77	6.42	6.04	6.43
Eu	1.05	1.08	1.42	1.44	1.31	0.98	0.97	0.41	0.16	1.32	1.16	1.10	0.81	0.39	0.30
Gd	2.50	3.57	4.57	4.78	6.35	5.75	5.63	5.96	3.75	5.97	4.92	5.47	6.60	6.38	6.66
Dy	2.35	3.07	4.05	3.94	4.93	5.53	5.65	7.02	4.44	5.04	4.39	4.58	5.20	6.76	10.10
Er	1.29	1.57	2.30	2.14	2.57	2.90	3.15	4.21	2.65	2.23	1.57	1.87	2.35	3.27	5.68
Yb	1.37	1.65	2.10	2.02	2.49	2.67	3.12	4.32	2.87	2.46	2.61	2.38	2.70	4.46	7.29
Lu	0.19	0.23	0.38	0.34	0.37	0.41	0.50	0.63	0.41	0.42	0.39	0.37	0.36	0.74	1.18
Ref.	[a]	[a]	[b]	[b]											

*U data from Brandebourger (1984). Refs.: [a]Casillas (1989), [b]Fúster and Rubio (1980) REE data from this work, [c]Brandebourger (1984), [d]Pérez-Soba (1991), [e]Andonaegui (1990).

Additional analytical data are available upon request.

considered to be better than 0.15% (2 s.d.). ε_{Nd} values were calculated using the following bulk earth parameters: $^{143}Nd/^{144}Nd = 0.512638$; $^{147}Sm/^{144}Nd = 0.1967$. The 2 s.d. error on ε_{Nd} calculations is ± 0.4. Nd. T_{DM} ages were calculated using the formula of Liew and Hofmann (1988), assuming $(^{143}Nd/^{144}Nd)_{DM} = 0.513151$, $(^{147}Sm/^{144}Nd)_{DM} = 0.219$, $(^{147}Sm/^{144}Nd)_{CC} = 0.12$.

All the Sr–Nd isotopic data are listed in Table 3. This includes eight metamorphic country-rocks from

PI granites			PS granites								
La Pedriza			Mora–Las Ventas				Alpedrete		El Cardin		HM
EX-203	87059	67065	80910	93458	93453	80913	95915	95916	Y-85	Y-81	Y-82
74.02	75.12	75.87	69.79	71.62	75.94	76.08	69.52	69.67	73.22	74.43	75.99
0.17	0.01	0.02	0.46	0.24	0.02	0.04	0.41	0.39	0.19	0.16	0.03
13.57	12.85	13.01	15.43	14.42	13.56	13.54	15.08	14.95	13.84	13.03	12.92
0.28	0.32	0.33	0.79	0.35	0.20	0.13	3.04	2.90	1.85	1.83	1.09
1.41	0.48	0.64	2.44	1.94	0.62	0.34					
0.05	0.03	0.03	0.06	0.03	0.04	0.05	0.04	0.05	0.02	0.01	0.02
0.04	0.01	0.06	0.54	0.58	0.05	0.09	0.97	0.95	0.44	0.33	0.07
0.91	0.43	0.48	2.15	1.20	0.40	0.27	2.45	2.45	1.11	1.24	0.52
3.56	4.24	4.12	3.39	3.41	3.79	3.37	3.33	3.30	3.35	3.13	3.62
5.04	4.28	4.50	3.92	4.44	4.08	4.48	3.96	3.82	4.60	4.60	4.75
0.02	0.08	0.12	0.19	0.32	0.16	0.11	0.16	0.15	0.13	0.10	0.07
0.65	0.83	0.35	0.81	1.22	0.94	0.67	0.85	1.18	1.06	0.97	0.76
99.83	98.68	99.52	99.97	99.77	99.79	99.76	99.81	99.81	99.81	99.83	99.84
1.05	1.04	1.04	1.12	1.14	1.19	1.24	1.06	1.07	1.11	1.05	1.07
369	1	4	559	236	12	11	477	500	284	192	26
247	516	405	201	246	399	297	175	182	254	236	327
56	1	1	131	67	8	12	172	173	70	44	11
53	136	67	33	20	9	15	26	21.8	26	66	40
	66	64	143	81	13	68	120	122	94	110	56
	44	27	12	10	7	8	11	10	8.6	9.2	7.9
25	27	16		5	4		11	10	12	22	13
1.04*								4.0*	3.01	5.48	12.7
33				16	4		34	31	151	19	6
10				74	67		74	8	70	81	
7				8	5		8	10	4	6	7
32.60	12.55	9.22	26.74	17.57	2.41	3.76	28.49	27.92	20.18	28.13	11.35
69.00	46.01	27.33	58.19	35.28	6.91	10.03	61.35	59.07	43.88	63.92	27.73
32.00	22.58	16.64	27.76	17.22	3.49	4.87	28.15	27.15	20.45	30.81	14.23
7.70	12.52	7.99	6.15	4.31	1.28	1.77	6.07	5.96	4.68	8.56	4.33
0.50	0.10	0.10	1.14	0.58	0.11	0.01	0.93	0.94	0.497	0.43	0.101
7.10	14.83	10.05	5.62	3.95	1.37	1.56	5.31	4.99	4.08	8.00	4.32
8.00	19.25	12.87	5.00	3.54	1.60	2.11	4.88	4.39	4.44	10.58	6.44
4.60	10.19	7.21	2.64	1.75	0.75	1.21	2.39	2.00	2.38	6.08	3.84
4.40	10.61	6.63	2.85	1.77	1.10	1.78	2.18	2.16	2.76	6.50	4.58
0.60	1.58	1.06	0.37	0.23	0.14	0.24	0.33	0.29	0.42	0.91	0.65
c	d	d	e			e					

Barbero et al. (1995) and a gabbroic sample from El Tiemblo from Casillas et al. (1991).

5. Chemical characterization

5.1. Major elements

The basic and intermediate rocks exhibit a wide range of chemical composition from gabbros to granodiorites (SiO_2 = 52 to 62 wt.% and, exceptionally, up to 70 wt.% in granodioritic facies of La Ventosilla pluton; MgO = 8.6 to 1.1 wt.%). On a SiO_2 vs. K_2O diagram (Fig. 2) they plot in the medium K sub-alkaline fields or on the boundary between this and the high K calc-alkaline series. The general chemical features of the basic and intermediate rocks are typical of the calc-alkaline series with metaluminous compositions being the most abundant, and

Table 3
Sr–Nd isotopic data for the Spanish Central Region metamorphic rocks, PI and PS granites

Sample	Rock type	[†]Age (Ma)	Rb (ppm)	Sr (ppm)	^{87}Rb/^{86}Sr	^{87}Sr/^{86}Sr	±2σ	(^{87}Sr/^{86}Sr)$_t$	Sm (ppm)	Nd (ppm)	^{147}Sm/^{144}Nd	^{143}Nd/^{144}Nd	±2σ	(^{143}Nd/^{144}Nd)$_t$	ε_{Nd}^t	[§]T_{DM}
93202*	Granulite	300	226	275	2.3788	0.73084	3	0.72068	10.07	53.81	0.1186	0.511894	8	0.511661	−11.5	1.93
93198*	Granulite	300	175	237	2.1430	0.72757	3	0.71842	11.05	54.80	0.1219	0.511878	7	0.511661	−12.0	1.93
93208*	Granulite	300	142	248	1.6586	0.72600	2	0.71892	10.88	54.17	0.1214	0.511857	6	0.511619	−12.4	1.99
90961*	Granulite	300	112	170	1.9053	0.72952	3	0.72139	10.30	50.91	0.1223	0.511871	6	0.511631	−12.1	1.97
92196*	Pelite	300	148	220	1.9217	0.72806	3	0.71986	11.70	56.04	0.1253	0.512032	7	0.511786	−9.1	1.73
77758	Pelite	300	146	140	3.0288	0.73531	3	0.72238	8.27	38.87	0.1286	0.511864	6	0.511719	−12.5	1.84
92194*	Pelite	300	174	129	3.9083	0.73301	3	0.71633	7.02	32.33	0.1312	0.511990	7	0.511611	−10.1	2.00
92199*	Pelite	300	179	95	5.4969	0.74084	2	0.71737	7.91	36.12	0.1324	0.511979	3	0.511732	−10.4	1.82
VO-16	Orthogneiss	300	66	121	1.5793	0.72338	5	0.71664	10.24	53.25	0.1162	0.512133	9	0.511905	−6.8	1.55
VO-19	Orthogneiss	300	122	182	1.9417	0.72359	9	0.71530	8.72	39.07	0.1349	0.512147	6	0.511882	−7.2	1.62
92193	Orthogneiss	300	245	87	8.2177	0.76281	3	0.72773	10.62	48.30	0.1329	0.512294	5	0.512033	−4.3	1.38
T-370	Orthogneiss	300	200	107	5.4336	0.74623	3	0.72303	6.07	24.99	0.1468	0.512187	6	0.511899	−6.9	1.62
VI-3	Orthogneiss	300	376	14	82.1418	1.29063	4	0.93996	1.97	5.49	0.2169	0.512306	6	0.511880	−7.3	1.78
92566*	Paragneiss BIR	300	105	196	1.5450	0.72030	3	0.71370	7.35	33.09	0.1343	0.512193	5	0.511929	−6.3	1.52
83535**	El Tiemblo	322	39	172				0.70765	3.04	12.09					−4.6	
60864	Ventosilla PS-types	300	74	369	0.5830	0.71136	2	0.70887	5.56	25.97	0.1294	0.512206	6	0.511952	−5.8	1.48
95916	Alpedrete	300	164	155	3.0659	0.72202	3	0.70893	5.96	27.15	0.1327	0.512189	7	0.511928	−6.3	1.52
76873	C. Mediana	291	184	106	5.0385	0.73057	13	0.70971	5.27	22.15	0.1438	0.512197	6	0.511923	−6.6	1.54

Y-81	Cardin	300	178	40	12.8668	0.76850	2	0.71357	8.56	30.81	0.1679	0.512255	7	0.511925	−6.4	1.52
Y-82	Hoyo Manz	300	222	7	97.6257	1.02018	4	0.60340	4.33	14.23	0.1839	0.512316	16	0.511955	−5.8	1.48
Y-85	Cardin	300	135	55	7.1563	0.74975	3	0.71920	4.68	20.45	0.1383	0.512209	7	0.511937	−6.1	1.50
77931		320	168	171	2.8425	0.72280	3	0.70985	8.70	43.52	0.1208	0.512189	6	0.511952	−5.7	1.48
80910	Mora−Ventas	320	199	128	4.4949	0.73013	6	0.70966	6.15	27.76	0.1339	0.512191	9	0.511910	−6.2	1.52
80212	Mora−Ventas	320	245	88	8.0486	0.74829	6	0.71163	4.97	21.02	0.1429	0.512189	7	0.511890	−6.6	1.55
80913	Mora−Ventas	320	300	13	67.8473	1.00099	13	0.69199	1.77	4.87	0.2197	0.512364	8	0.511904	−6.3	1.53
	PI-types															
92460	Villacastin	323	131	143	2.6519	0.71961	2	0.70742	7.46	34.44	0.1309	0.512214	8	0.511937	−5.6	1.48
92444	La Granja	299	190	96	5.7299	0.73549	2	0.71111	7.78	32.13	0.1463	0.512208	7	0.511922	−6.5	1.53
95922	Atalaya Real	284	143	131	3.1622	0.72366	3	0.71088	7.98	44.04	0.1395	0.512170	7	0.511966	−6.0	1.48
96029	Atalaya Real	284	179	104	5.0081	0.73362	3	0.71338	6.55	28.02	0.1413	0.512226	6	0.511963	−6.0	1.48
96024	Atalaya Real	284	250	37	18.7674	0.78728	3	0.71144	6.48	25.53	0.1534	0.512282	7	0.511997	−5.4	1.43
55718	La Cabrera	310	138	187	2.1351	0.71859	2	0.70917	5.85	39.85	0.0887	0.512164	8	0.511984	−5.1	1.42
56205	La Cabrera	310	149	158	2.7416	0.72125	2	0.70915	7.77	35.91	0.1308	0.512174	7	0.511909	−6.5	1.54
55702	La Cabrera	310	226	41	15.8775	0.77566	2	0.70561	6.04	20.86	0.1750	0.512275	7	0.511920	−6.2	1.52
56201	La Cabrera	310	298	13	68.3745	0.98199	2	0.68034	6.43	19.64	0.1979	0.512335	7	0.511933	−6.0	1.50

∗ Data from Barbero et al. (1995).

∗∗ Data from Casillas et al. (1991).

[†] The ages for the PS and PI granites are their crystallization ages. When no isochron is available (see Table 1), isotopic ratios were calculated at 300 Ma. The age against the other samples is the time to which the measured isotopic ratios have been corrected in the table.

[§] Model ages for the PS and PI granites are calculated using their crystallization age. The crystallization age for the orthogneisses is 500 Ma. The Sm/Nd of the metasediments are close to that of the average crust used in the model age calculation; thus, the value used for the 'crystallization age' in the calculation does not unduly influence the model age. A value of 650 Ma has been used.

only the most differentiated rocks being slightly peraluminous.

PI and PS granitoids have a range in silica content from 63.5% to 77.6 wt.%, although the majority are in the range 67.8% to 76.5%. On a SiO_2 vs. K_2O diagram, they plot in the high-K field (Fig. 2). Almost all these granites are peraluminous; PS types are clearly peraluminous, whereas PI types are slightly peraluminous or metaluminous (Fig. 3). The

greater peraluminosity of the PS types reflects their slightly lower CaO and Na_2O contents compared to PI types. The more restricted range of P_2O_5 contents of the PI types are also remarkable (Fig. 2). These features are common in granitic series with different degrees of Al saturation (Bea et al., 1992). Both PI and PS types show similar evolutionary trends with increasing silica contents: FeO_t, MgO, MnO, TiO_2, Al_2O_3, CaO and P_2O_5 decrease, K_2O increases and
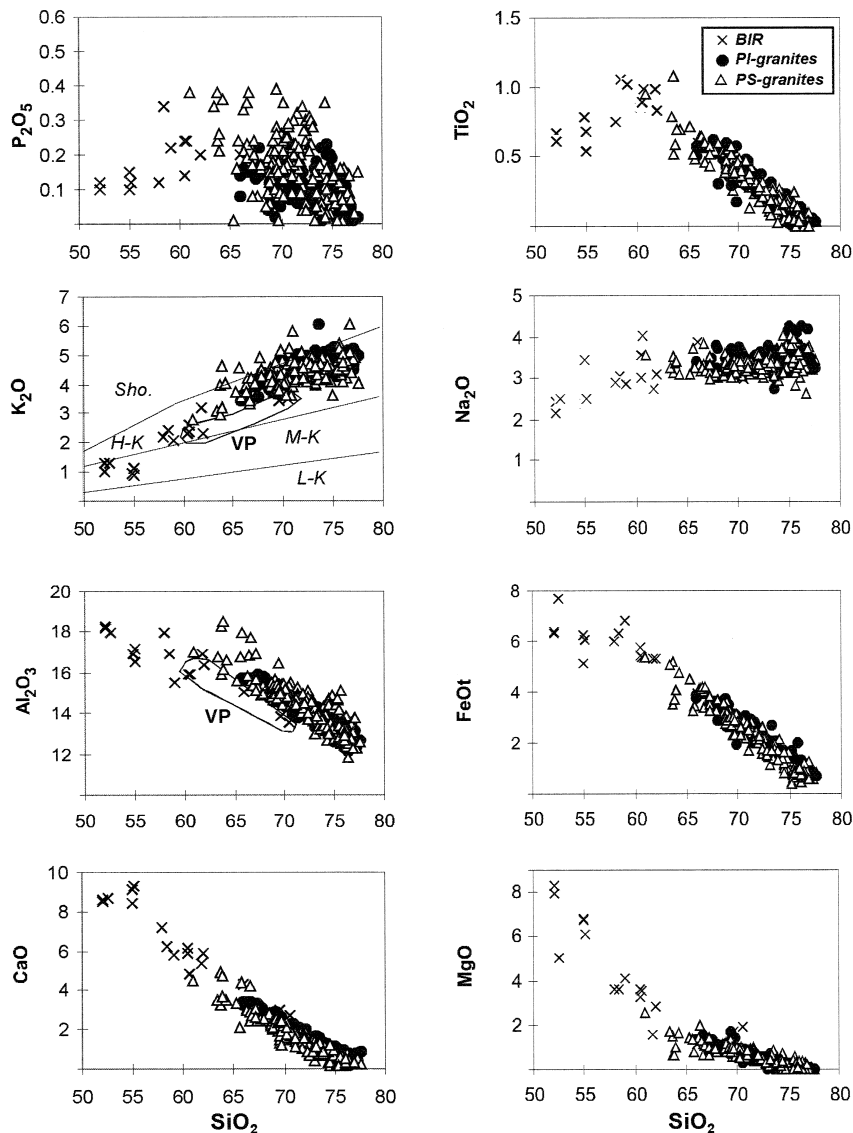
Fig. 2. Harker variation diagrams for selected major elements for granites from the SCR. Crosses = basic and intermediate rocks; black dots = PI granites; open triangles = PS granites. In some diagrams, compositional fields for La Ventosilla pluton are marked (VP). Fields on K_2O vs. SiO_2 diagram are Sho = shoshonitic, H-K = high K, M-K = medium K, L-K = low K (Rollinson, 1993).
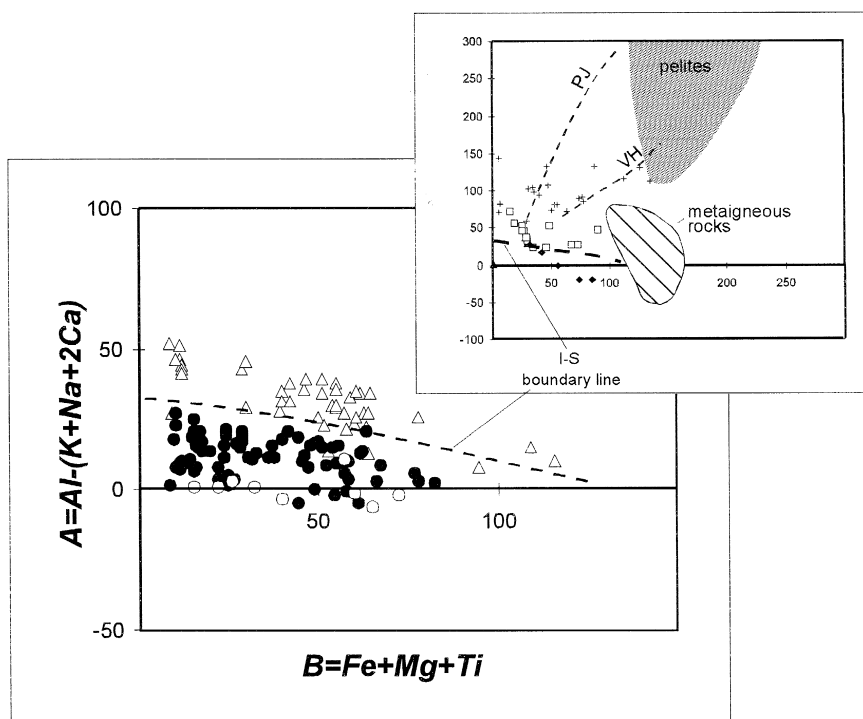
Fig. 3. A–B diagram after Debon and Le Fort (1983) for selected PI and PS granites from the SCR. PI-types: open circles = Atalaya Real granite; black dots = Navas del Marqués granite; PS-types: open triangles = Mora granites. I–S boundary line is drawn from I- and S-types data from the Lachlan Fold Belt (White and Chappell, 1989). Inset shows the fields of experimental granitic liquids produced from diverse pelitic and meta-igneous protoliths: crosses = pelite-derived granitic liquids; dotted lines show two different trajectories of liquids from progressive melting of pelitic protoliths (PJ = Patiño Douce and Johnston, 1991; VH = Vielzeuf and Holloway, 1988). Squares = meta-igneous-derived liquids (Holtz and Johannes, 1991; Conrad et al., 1988). Black diamonds are experimental liquids from progressive melting of a metaluminous igneous protolith (Conrad et al., 1988).

Na_2O shows little change (Fig. 2). The trend of the basic and intermediate rocks is almost collinear with the PI–PS trend for some major elements (e.g., CaO and FeO_t), but there is a marked inflection between the two trends for MgO, TiO_2 and P_2O_5 (Fig. 2). Other elements such as Al_2O_3, K_2O and Na_2O are lower in the basic and intermediate rocks, although the most differentiated samples join the granite trends (Fig. 2).

In Harker diagrams, there is a compositional gap between the basic–intermediate rocks and the PI granites (62–67 wt.% SiO_2). Nevertheless, some scarce foliated PS facies (mainly those that form part of the Cebreros pluton interacting with El Tiemblo basic–intermediate types, Casillas, 1989) join the basic–intermediate rocks with the general granite trend. The Ventosilla tonalite–granodiorite pluton is markedly off the general trend in some plots (Fig. 2).

5.2. Trace elements

The basic and intermediate rocks have LILE contents around 50 to 300 times chondritic values for Rb and Ba, and about 30 times for Sr. The Sr contents of the basic and intermediate rocks are lower than those typical of basic and intermediate calc-alkaline series rocks, for example, from Caledonian continental margins (Thompson et al., 1984), and even from Hercynian quartz–diorites (Shaw et al., 1993). In trace element chondrite-normalised diagrams (Fig. 4), the basic and intermediate rocks of the area show negative anomalies in Ba, Nb, Sr, P, and Ti, relatively fractionated patterns $(Rb/Lu)_n = 20$, and moderate to low contents of certain HFSE (Nb, Zr, Y). The high LILE/HFSE element ratios and the major element contents are typical of calc-alkaline magmas (see also Casillas, 1989). REE patterns show

a moderate fractionation ($La/Yb_n = 10$) and either a slight negative or positive Eu anomaly ($Eu/Eu* = 1.19$ to 0.85)(Fig. 5). The REE pattern with the positive Eu anomaly corresponds to the most primitive gabbro (Table 2 and Fig. 5); the negative Eu anomalies suggest plagioclase fractionation has occurred, which is consistent with the low Sr contents of the rocks.

PI and PS granite types have very similar contents for most of the trace elements and also similar trace element ratios (Figs. 4 and 6, Table 2). Chondrite-normalised trace element patterns have negative anomalies in Ba, Nb, Sr, P, and Ti that become increasingly marked towards the most felsic and fractionated granitic facies; such trends are typical of
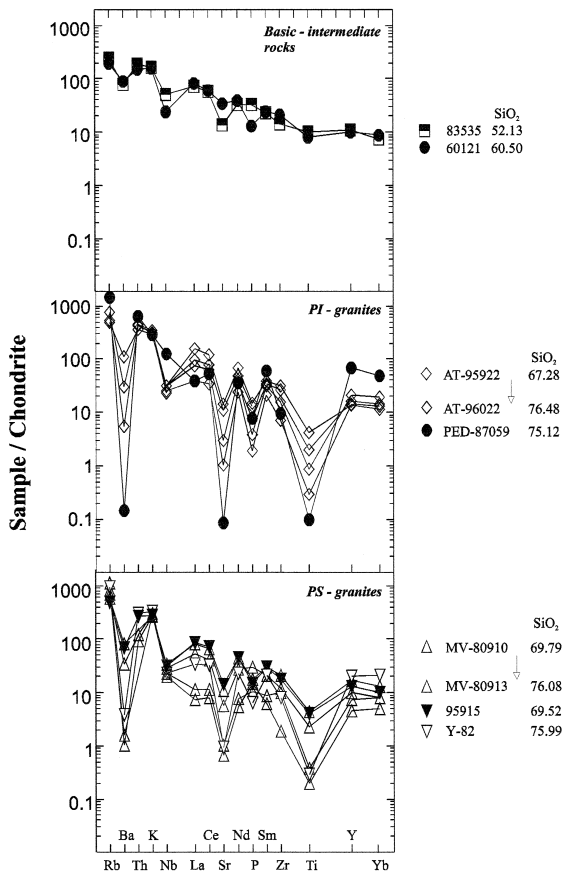
Fig. 4. Chondrite-normalized trace element patterns for basic/intermediate rocks and selected PS and PI granites. In PI-granites plot, AT = Atalaya Real pluton; PED = La Pedriza pluton. In PS-granite plot, MV = Mora–Las Ventas pluton; data from Table 2. Normalizing values from Thompson et al. (1984).
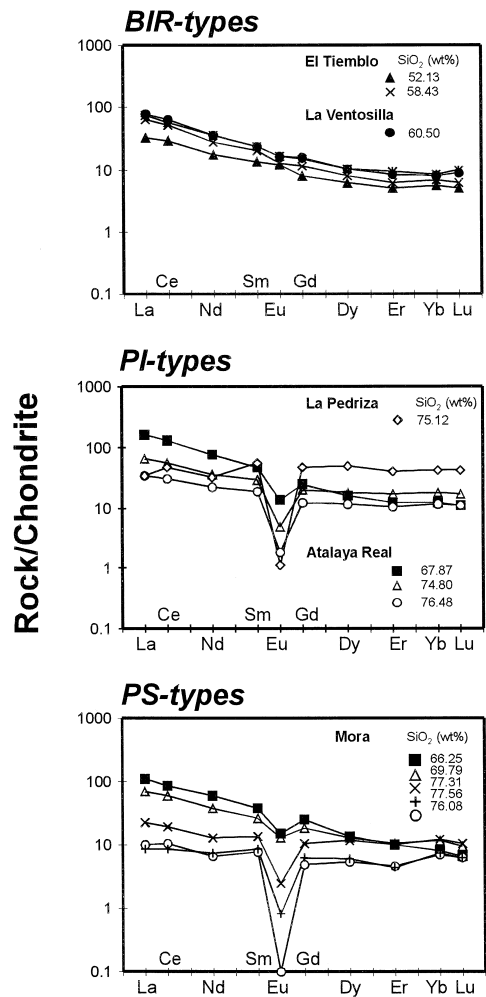
Fig. 5. Chondrite-normalized REE patterns for basic/intermediate rocks (BIR) and selected PS and PI granites. Normalizing values from Masuda et al. (1973).

collisional peraluminous granitoids (Thompson et al., 1984). The LILE show common behaviour; compatible for Ba and Sr, whereas Rb is incompatible (Fig. 6). REE patterns within individual plutons vary from LREE-enriched ($La/Yb_n = 20$–10) with slight negative Eu anomalies ($Eu/Eu* = 0.6$–0.5) towards flat patterns and large negative Eu anomalies (wing-shaped patterns with $La/Yb_n = 3$–1.4 and $Eu/Eu* = 0.3$–0.01)(Fig. 5). Some PI plutons show a strong enrichment in Th, Y, Nb, and HREE for samples with silica in the range between 74 and 76 wt.% (Fig. 6).
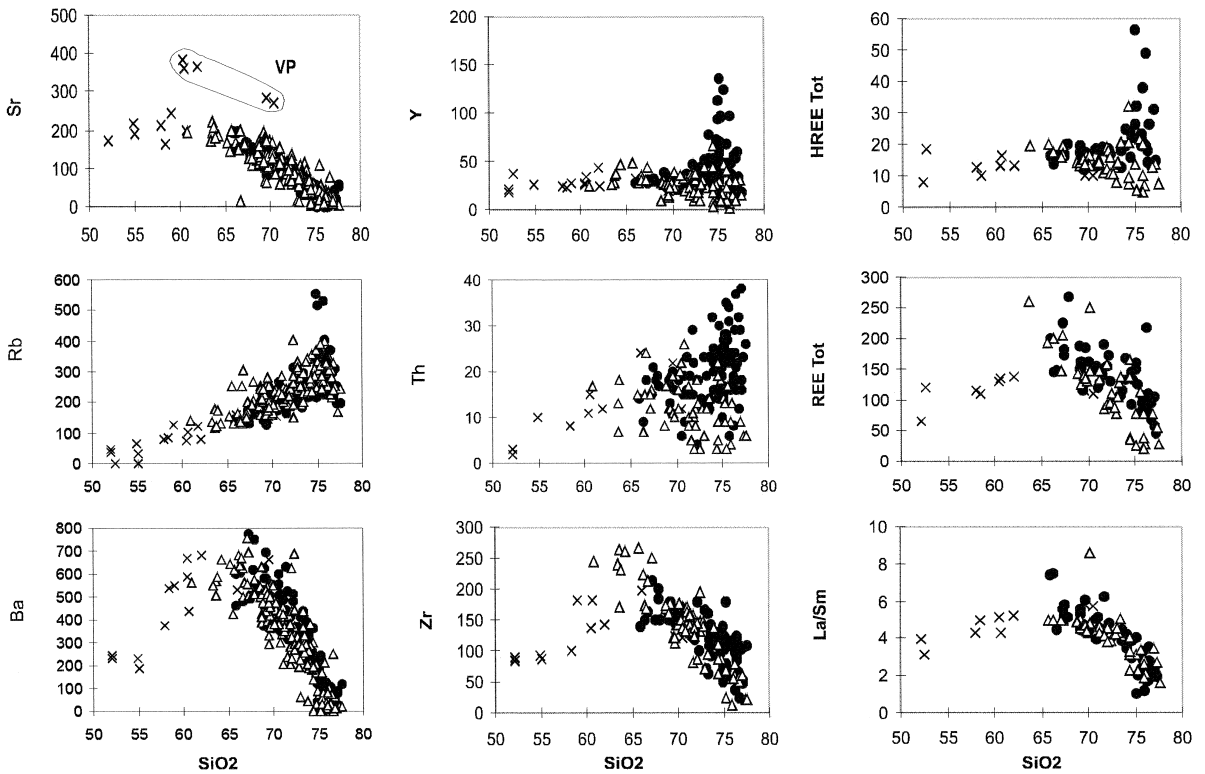
Fig. 6. Harker variation diagrams for selected trace elements and trace element ratios for granites from the SCR. Symbols as in Fig. 2.

As with the major elements, the trace elements of the basic and intermediate rocks sometimes plot collinearly with the granites, but in most of the plots, there is an inflection linking both general trends (Figs. 2 and 6). For elements such as Ba, Sr, Zr, Nb, and the REE, the most evolved basic rocks and some silica-poor PS granites follow a bell-shaped pattern with a maximum concentration of these elements in rocks in the range 60–67 wt.% SiO_2 (Fig. 6). For other trace elements, all the groups follow the same downward or upward trend. La Ventosilla pluton plots outside these general trends in some Harker diagrams (Fig. 6).

5.3. Sr–Nd and other isotopic data

Table 3 and Fig. 7 show Sr and Nd isotopic data for selected samples of the SCR granites. These granites show a narrow range of negative ε_{Nd}^i values (−5.1 to −6.6). Initial $^{87}Sr/^{86}Sr$ ratios vary from 0.7073 to 0.7193 with most between 0.708 and

0.712. There are no significant differences in initial Sr–Nd isotopic signatures between the PI and PS granite types (Fig. 7).

The most striking feature of Fig. 7 is the horizontal trend exhibited by the whole data set of peraluminous granites. This pattern differs greatly from the steeply-sloped fields documented for the Lachlan Fold Belt batholiths studied by McCulloch and Chappell (1982) or the Andean batholiths studied by Rogers and Hawkesworth (1989), which form trends which curve from crustal values towards positive initial ε_{Nd} and low initial $^{87}Sr/^{86}Sr$ indicating the involvement of a depleted mantle component. The striking feature of the initial Sr and Nd isotopic data of the granites from the SCR, especially in comparison with data from continental margin batholiths, is the lack of indication of any mantle contribution. This is also shown in Hercynian areas where peraluminous granites are dominant: e.g., the French Massif Central (Pin and Duthou, 1990) or the Bohemian Massif (Liew et al., 1989), although Janousek et al.
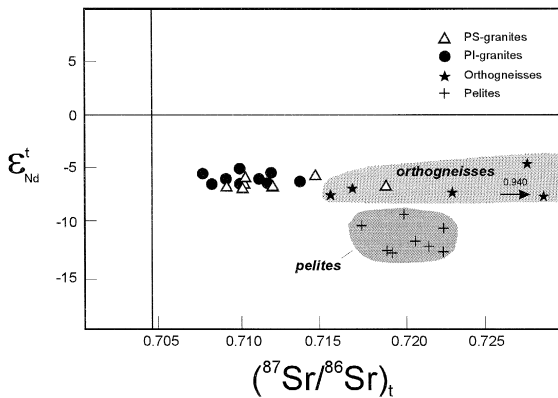
Fig. 7. Initial $^{87}Sr/^{86}Sr$ vs. initial ε_{Nd} plot for SCR granites and metamorphic rocks. Metamorphic rocks (orthogneisses and pelites) have initial values calculated assuming an average age of 300 Ma.

(1995) have argued that similar isotopic signatures in mafic potassic lithologies from the Bohemian Massif reflect enriched mantle sources. In the case of the Spanish Central System, however, such lithologies are absent.

Several highly-fractionated leucogranites with high silica contents ($> 75\%$ SiO_2) show anomalous isotopic compositions, having impossibly low initial Sr ratios (0.693–0.600, Table 3).The most felsic rocks have very low Sr contents and are therefore, the most sensitive to disturbance of the Rb–Sr system. Such low apparent initial Sr isotopic ratios in felsic rocks are usually ascribed to post-magmatic isotopic alteration (e.g., Kwan et al., 1992; Moreno-Ventas et al., 1995), or to interaction or mixing with other melts in open magmatic systems (Christiansen and DePaolo, 1993). Alternatively, because these rocks have the highest $^{87}Rb/^{86}Sr$, even small variations in the apparent age of the plutons may result in significant differences in the calculated initial $^{87}Sr/^{86}Sr$. In the case of sample 80913 from the Torcón intrusion, if an age of 300 Ma is used instead of 320 Ma, then the initial $^{87}Sr/^{86}Sr$ becomes $\sim$ 0.711, comparable with the related Mora granites.

In Fig. 7, isotopic data from the regional metamorphic rocks are plotted together with those of the granites. Data for the metamorphic rocks have been age-corrected assuming an age of 300 Ma (Table 3). The low Rb/Sr ratios shown by the rocks have only a minor effect on this calculation. The orthogneisses show a wide range of $(^{87}Sr/^{86}Sr)_{300}$ values, with the highest values in the more leucocratic facies (up to 0.93996, sample VI-3, Table 3). In contrast, the metapelites show a more restricted range of $(^{87}Sr/^{86}Sr)_{300}$ values (0.7164–0.7224, Table 3). Both materials show much less variation in $(\varepsilon_{Nd})_{300}$ values, which is a common feature of the Hercynian crust (Bickle et al., 1988). The orthogneisses have $(\varepsilon_{Nd})_{300}$ values between -4.3 to -7.3, whereas the metapelites have lower values from -9.1 to -12.5, as is also typical in the Hercynian Belt (Downes and Leyreloup, 1986; Downes and Duthou, 1988). A semi-pelitic paragneiss (sample 92566 of Table 3) has a Nd isotopic composition very close to that of the orthogneisses.

$(\varepsilon_{Nd})_{300}$ values of the orthogneisses are the same as the initial ε_{Nd} of the Hercynian granites which may suggest that they are a likely source. On the other hand, all the metamorphic rocks have higher $(^{87}Sr/^{86}Sr)_{300}$ values than the granites. Metamorphic rocks with lower $(^{87}Sr/^{86}Sr)_{300}$ are absent in the area.

Scarce published Pb and O isotopic data show that the PI and PS granites have similar values: $^{206}Pb/^{204}Pb = 18.24$–18.33, $^{207}Pb/^{204}Pb = 15.59$–15.62, $^{208}Pb/^{204}Pb = 38.15$–38.28 (Pérez-Soba, 1991) and $\delta^{18}O = 7.0$–7.9‰ (Aparicio et al., 1986). The coincidence of isotopic ratios as well as the similarity in trace element geochemistry suggest a similar source for the origin of the various granite types of the Spanish Central Region.

6. Petrogenesis and discussion

6.1. The role of crystal fractionation in the granitic magmas

The chemical variation in some of the granitic complexes of the area has been successfully modelled by fractional crystallization from relatively silica poor ($SiO_2 = 67$–69 wt.%) monzogranitic parental magmas (Casillas, 1989). Several facts support crystal fractionation at the pluton scale.

(1) Negative trends on incompatible (e.g., Rb) vs. compatible (Sr, Ba, Eu,...) element log–log diagrams characterize the chemical variation produced by crystal fractionation in granitic magmas (Cocherie et al., 1994). La Atalaya Real PI-type pluton has

been selected as an example of modelling the chemical variation in SCR granites by crystal fractionation (Table 4). A least-squares method using mineral phases identified in the pluton, mineral compositions determined by microprobe analyses, granodiorite sample 95922 as the starting material and leucogranite 96022 as the evolved magma, indicates that differentiation requires the fractionation of 47% plagioclase, 21% quartz, 17% biotite, 14% K-feldspar and some minor phases (apatite, ilmenite) with the proportions of removed solid vs. evolved melt of approximately 75/25. The $\sum R^2$ (sum of squares of oxide residuals) is 0.050 indicating a good degree of fit of the model to the data. Similar calculations for other PI or PS plutons are shown in Table 4. Lower degrees of fractionation (e.g., the felsic PI La Pedriza pluton) leave lesser amounts of cumulates, the compositions of which are similar to those of the granodiorites and monzogranites of the area (30–45% plagioclase, 20–30% quartz, and 12–30% K-feldspar). Using these mass balance constraints and mineral–liquid partition coefficients for dacitic and rhyolitic magmas (Nash and Crecraft, 1985; Arth, 1976),

trace element modelling for Ba, Rb, and Sr yielded values close to those observed in each pluton. Fig. 8 contains all the analyses from PS and PI plutons which does not correspond exactly to a unique evolutionary trend as they integrate data from different evolutionary trends. As can be deduced from the modelling of three intrusions: Atalaya Real, La Pedriza and Mora–Las Ventas plutons (Fig. 8), their parental magmas plot in different positions on the diagrams. So, different evolutionary paths in these diagrams could cross depending on the Ba–Rb and Sr–Rb composition of the parental magmas involved in each case. This heterogeneity explains why there is not a unique model for the LILE evolution and that any supposed 'liquid line-of-descent' for the SCR granites is in fact a bundle of overlapping lines-of-descent.

(2) The REE variation within individual plutons described above is typical of feldspar and accessory mineral (allanite, monazite, etc.) fractionation in granitic magmas (Cocherie et al., 1994)(Fig. 5).

(3) The models for fractional crystallization in Table 4 indicate that the most felsic leucocratic

Table 4
Crystal fractionation models for PI and PS granites from Central Spain

| Parental magma	Fractionated magma	Percent crystallization (residuals after major element calculation)	Major and accessory minerals and percent of fractionation assemblage
PI granites			
Atalaya Real granodiorite 95922	Atalaya Real leucogranite 96022	73% ($\sum R^2 = 0.050$)	47.2 Plg + 21.2 Q + 16.7 Bt + 14.3 Kf + 0.5 Ap + 0.1 Ilm
Navas monzogranite 76396	Peña–Madrid leucogranite 95159	51% ($\sum R^2 = 0.121$)	42.2 Plg + 23.8 Q + 17.7 Bt + 15.6 Kf + 0.5 Ilm + 0.11 Ap
Cabrera monzogranite 56205	Cabrera leucogranite 56201	78% ($\sum R^2 = 0.187$)	43.5 Plg + 27.4 Q + 14.3 Bt + 14.6 Kf + 0.4 Ap
Pedriza leucogranite EX-203	Pedriza leucogranite 87059	43% ($\sum R^2 = 0.020$)	30.1 Plg + 30 Q + 29.9 Kf + 9.5 Bt + 0.35 Ap + 0.17 Ilm
Granja monzogranite 92443	Granja granite 92439	40% ($\sum R^2 = 0.013$)	46.5 Plg + 24 Q + 15.5 Bt + 13.1 Kf + 0.78 Ap + 0.1 Ilm
PS granites			
Mora monzogranite 80910	Torcón leucogranite 80913	66% ($\sum R^2 = 0.118$)	43.8 Plg + 27 Q + 15.4 Bt + 13.2 Kf + 0.48 Ap + 0.14 Ilm
Alpedrete monzogranite ($n = 5$)	Cabeza Mediana leucogranite EX-191	72% ($\sum R^2 = 0.132$)	42 Plg + 27.6 Q + 15.8 Bt + 12.6 Kf + 1.5 Cdta + 0.34 Ap + 0.14 Ilm
Hoyo Pinares monzogranite 83571	HP leucogranite 86177	51% ($\sum R^2 = 0.0782$)	41.3 Plg + 23.8 Q + 21.1 Bt + 12.6 Kf + 0.43 Ilm + 1 Ap
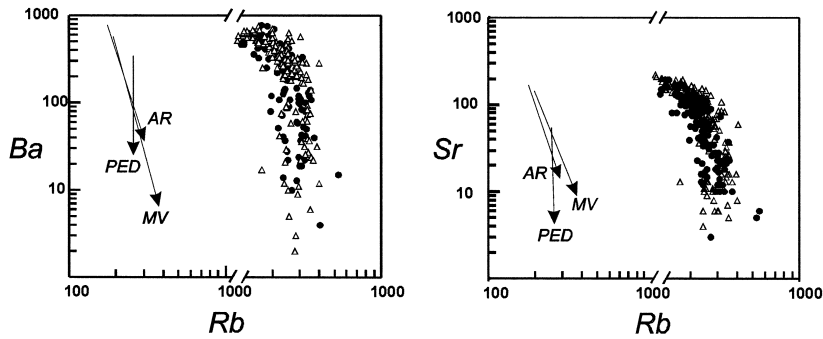
Fig. 8. Plots of Rb vs. Ba and Sr on a log–log scale for the SCR granites. Some modelled crystal fractionation trend for Atalaya Real (AR), La Pedriza (PED) and Mora–Las Ventas (MV) are shown for comparison. Symbols as in Fig. 2.

facies rarely represent more than 20–30% of residual magma which is similar to the proportion of outcropping felsic rocks in relation to less evolved granites. Moreover, the most felsic leucogranites appear in the central parts of the plutons, closely-related to the more acidic monzogranitic varieties.

(4) The fact that Rb–Sr whole-rock isochrons can be obtained for most of the plutons (Table 1) suggests that each magma was homogeneous with respect to Sr isotopes. This, coupled with Nd isotopic homogeneity within individual intrusions (Table 3), is consistent with a closed system evolution via crystal fractionation for each pluton.

The PI and PS granites are not related by simple crystal fractionation processes. The parental magmas of each of the granitic series show a marked contrast in peraluminosity (Fig. 3); given that the isotopic data suggest that both series were derived from similar sources, the contrast in peraluminosity between them is most probably related to different partial melting conditions. In partial melting experi-

ments on crustal rocks, feldspar stability fields change markedly with respect to P–T conditions, indicating that the peraluminosity of the partial melt is very sensitive to the depth of melting within thickened continental crust (Patiño Douce, 1994). The parental magmas generate two different series which evolve with parallel trends (Fig. 2). The two granite types, PI and PS, are never found in the same pluton. There is some convergence of the evolutionary trends towards the most felsic varieties of the PI and PS types, which is also reflected in their AFM mineralogy (Villaseca and Barbero, 1994a). However, the different role of accessory phases in the PI and PS types leads to contrasting chemical trends, for certain trace elements such as Th, Nb, Y, and HREE. Certain felsic PI types show a marked enrichment in Th, Y, (Nb in La Pedriza pluton, see Table 2) and HREE (Fig. 6), which is typical of granitic series where fractionation is controlled by allanite (slightly peraluminous granitic series; Förster and Tischendorf, 1994). These enrichments also imply that both mon-
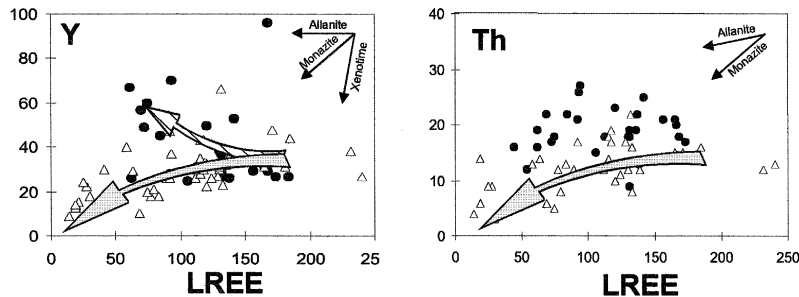

Fig. 9. Y vs. LREE and Th vs. LREE diagrams for PI and PS granites from SCR in which it include vectors showing the effect of accessory phases (allanite, monazite, xenotime) fractionation. See text for further explanation.

azite and xenotime played a role in the evolution of the PI series. The dominant role of allanite in controlling the content of certain HFSE in the PI plutons is suggested by trace element modelling (Fig. 9). Allanite is never found in the PS plutons in which the most abundant REE-bearing phase is monazite and more rarely xenotime.

It is noticeable that the incompatible behaviour of Th, Y, and HREE in some PI granites is very characteristic of weakly peraluminous acid magma (Champion and Chappell, 1992), with the relative magnitude in the variation of these elements being strongly granite type-dependent (see La Pedriza pluton as the richest HFSE + HREE granite). Although the high Nb, Y, and HREE contents of some PI granites resemble those of A-type granites, as documented by Champion and Chappell (1992) for similar felsic peraluminous I-types in northern Queensland (Australia), the PI granites of Sierra de Guadarrama have Nb, Y and HREE contents that increase with progressive fractionation from baseline levels more typical of I-type granites.

6.2. The role of the associated basic magmatism

The overwhelming difference in volume of the granites compared to the basic rocks, strongly suggests a limited mantle contribution to the origin of the peraluminous granites, via either crystal fractionation or basic–acid magma mixing.

In the studied region, only one of the basic massifs has a local marginal facies of gabbroic composition (El Tiemblo massif, Casillas, 1989) (see also Table 1). This massif contains a large quantity of granitic veins and brecciated facies indicating that hybridization between basic and more acid magmas occurred. Also, these gabbroic rocks do not show any primary mantle-derived signature (Table 2); Mg, Cr, and Ni, are very low, suggesting that significant fractionation has occurred. Casillas et al. (1991) reported an initial $^{87}Sr / ^{86}Sr$ ratio of 0.7076 for the El Tiemblo gabbros with initial ε_{Nd} of -4.5; oxygen isotopic values of this massif are $\delta^{18}O = 7.0‰$ (Aparicio et al., 1986). In the western Spanish Central System areas, the isotopic variability shown by the scarce basic massifs indicates that they also contain crustal components (Moreno-Ventas et al., 1995).

In most of the PS and PI monzogranites, microgranular enclaves are conspicuous. In general, these enclaves are interpreted as hybrid rocks. It has been shown that the isotopic composition of the enclaves resembles that of the immediate host granite, suggesting that the isotopic re-equilibration between the enclave and its host has occurred (Stephens et al., 1991). However, Sr and Nd isotopic differences have also been observed in microgranular enclaves from nearby granitic areas (Moreno-Ventas et al., 1995; Pinarelli and Rottura, 1995), implying that equilibration is not always achieved, at least within large enclaves. Although such enclaves may have partially equilibrated, this isotopic disequilibrium provides some constraints on the isotopic signature of the mafic precursor. In both cited studies, the basic end-member tends to have a Sr–Nd isotopic composition close to bulk earth values. In SCR plutons, some marginal facies of granodioritic composition, which are also usually richer in mafic microgranular enclaves, have initial Nd isotopic compositions slightly more positive than that of the main granite body (see analysis 55718 in Table 3), suggesting limited basic–acid magma mixing. Moreover, within individual plutons (e.g., Atalaya Real and La Cabrera) there are no systematic changes in initial isotopic ratios with chemical composition, and therefore, the chemical variability within the plutons is unlikely to be caused by mixing processes. Thus, the overall geochemical variability of each of the granitic series is satisfactorily explained by crystal fractionation from a granodiorite/monzogranite parental magma. This is consistent with the assumption that large-scale mixing of felsic and mafic magmas is unlikely because of their contrast in chemical composition and physical parameters such as viscosity and temperature (Sparks and Marshall, 1986). Nevertheless, limited-scale mixing between the coeval basic and acid magmas could explain the more evolved intermediate rocks in the basic massifs, the mixed marginal facies found in some plutons, and the presence of mafic microgranular enclaves. This is shown in the Harker diagrams where the mixed facies plot in the inflection region at around 62–67% SiO_2 (Fig. 6), indicating limited interaction between a basic-derived intermediate magma and certain parental granodioritic liquids of the PS series, as also stated by

Poli et al. (1996) and Di Vincenzo et al. (1996) in other areas.

The isotopic data are also consistent with a restricted contribution of the basic magmas in the overall chemical variability of the granitic series. A mixing model using a basic end-member with a bulk earth Sr–Nd isotopic composition (as used by Moreno-Ventas et al., 1995) has several limitations. In Fig. 10a, mixing lines between bulk earth values and the two types of metamorphic rocks of the area are plotted. It is apparent that the mixing line involving the metasediments does not pass through the field of the granites, largely because of the lower $(\varepsilon_{Nd})_{300}$ values of the potential contaminant. The mixing line involving the orthogneisses provides a closer fit to the data, with the granites containing between 25–50% of the mantle component. Such a high mantle contribution does not seem to be realistic as basic material is almost absent in the entire Central Iberian zone to which the SCR belongs.

AFC-style crustal contamination of a mantle-derived magma with a bulk earth isotopic composition by both the pelitic and meta-igneous lithologies has also been considered. All the models use D_{Sr} of 1.5 and D_{Nd} of 0.5, values broadly consistent with the observed geochemical behaviour of Sr and Nd in these rocks (Fig. 6). Using a meta-igneous contaminant, it is apparent in Fig. 10b that only those models

with r (assimilation rate to fractionation rate) in the range of 0.5 to 0.8 fit the observed isotopic data of the granites (compare curves 1–3 and 2–4 of higher r values, Fig. 10b). However, thermal considerations have shown that assimilation rates in excess of 0.2 to 0.3 seem to be unrealistic unless the basic magma is superheated and the wall rock is at a temperature close to that of its solidus (DePaolo, 1981). Conse-
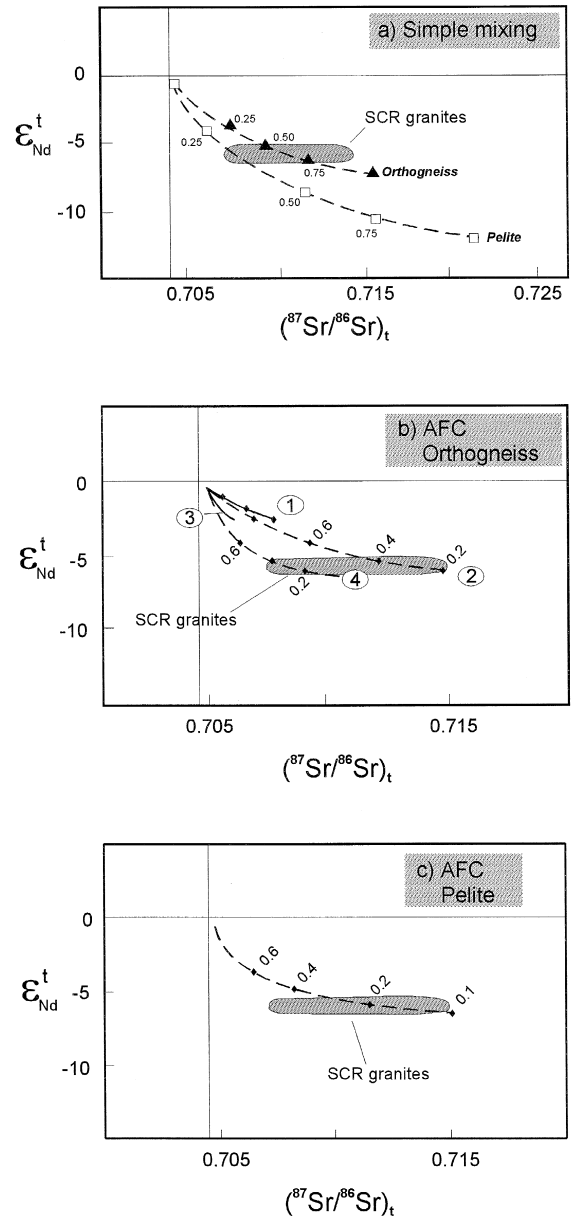
Fig. 10. (a) Upper diagram: initial ^{87}Sr/^{86}Sr vs. initial ε_{Nd} plot showing mixing lines between a bulk earth mantle and an average orthogneissic end-members (black triangles) and a bulk earth mantle and average pelite end-members (open squares). Numbers refer to different mixing proportions of the crustal end-members. Mantle end-member composition is $(^{87}$Sr/^{86}Sr$)_t = 0.70465$, initial $\varepsilon_{Nd} = -0.63$, Sr = 366 ppm, Nd = 26 ppm; orthogneissic end-member $(^{87}$Sr/^{86}Sr$)_t = 0.71532$, initial $\varepsilon_{Nd} = -7.21$, Sr = 182 ppm, Nd = 39.07 ppm; pelitic end-member $(^{87}$Sr/^{86}Sr$)_t = 0.721$, initial $\varepsilon_{Nd} = -12$, Sr = 180 ppm, Nd = 45 ppm. (b) Middle diagram: initial ^{87}Sr/^{86}Sr vs. initial ε_{Nd} plot showing AFC models considering the same mantle and orthogneissic end-members as above. Lines 1 and 2 calculated for $D_{Sr} = 1.5$ and $D_{Nd} = 0.5$, full line (1) for $r = 0.2$ and dashed line (2) for $r = 0.6$. Lines 3 and 4 calculated for $D_{Sr} = 0.5$ and $D_{Nd} = 0.5$, full line (3) for $r = 0.2$ and dashed line (4) for $r = 0.6$. Tick marks on curves refer to different F values (F = fraction of magma remaining). (c) Lower diagram: $(^{87}$Sr/^{86}Sr$)_t$ vs. initial ε_{Nd} plot showing AFC model considering the same mantle and pelitic end-member as above. Dashed line calculated for $D_{Sr} = 1.5$, $D_{Nd} = 0.5$ and $r = 0.6$. Tick marks on curve refer to different F values.

quently, AFC-style contamination by the orthogneisses is considered to be an unlikely process to produce the isotopic signatures of the granites. Given the isotopic heterogeneity of both the pelites and the granitic melts derived from them (Barbero et al., 1995), the pelite-derived contaminant is unlikely to have a unique geochemical composition, and therefore, a perfect fit of the modelled trends through the data is not to be expected. Nonetheless, modelling involving such a contaminant produces a fit of the isotopic data for the granites similar to that of the meta-igneous contaminant using similar modelling parameters (Fig. 10c). However, the modelling indicates that large amounts of fractionation ($>60\%$, or conversely, small amounts of magma remaining, $F < 0.4$ in Fig. 10) are required to reproduce the isotopic composition of the granites. This, in turn, would lead to the generation of large proportion of cumulate basic–intermediate rocks, the evidence for which is completely absent within the SCR. Consequently, although modelling of AFC-style contamination may reproduce the isotopic variation found in the SCR granites, such results are at variance with geological considerations, and therefore, such processes considered unlikely to be the main cause of the geochemical variation seen in the granites.

6.3. Crustal protoliths and the lack of appropriate sources in terms of isotopic composition

The compositions of the least evolved PI and PS type granites are similar to those of the melts produced experimentally from meta-igneous rather than from pelitic protoliths (inset in Fig. 3 and references therein). This major involvement of meta-igneous protoliths in the genesis of the granites is also supported by the CaO and Na_2O contents of the granites which are higher than in pelite-derived magmas (Miller, 1985; Barbero and Villaseca, 1992). The Nd isotopic data of the orthogneisses in the present-day upper crust match those of the granites, although their Sr isotopic composition is clearly more radiogenic (Fig. 7). This absence of crustal protoliths with an appropriate Sr isotopic composition is a common feature in Hercynian areas, e.g., Pyrenees (Bickle et al., 1988), southern Armorican Massif (Bernard-Griffiths et al., 1985), Bohemian Massif (Liew et al., 1989). In some cases, where there is an abundance of

small basic massifs, it is possible to demonstrate that the absence of appropriate protoliths is due to interaction or mixing with mantle-derived magmas (Dias and Leterrier, 1994; Moreno-Ventas et al., 1995; Pinarelli and Rottura, 1995), whereas in others, unsampled crustal protoliths are invoked (Bernard-Griffiths et al., 1985).

In recent years, however, alternative explanations have been proposed. Bickle et al. (1988) showed that Sr isotopic signatures are strongly affected by high-grade metamorphism and anatexis, suggesting that metapelites (and orthogneisses) may maintain their major and trace element compositions, but that they may be strongly isotopically modified, depending on whether they equilibrate at lower or upper crustal levels. According to these authors, the aqueous fluids expelled during prograde metamorphism provoke homogenisation of the $^{87}Sr/^{86}Sr$ ratios in the rocks with the effect of lowering these ratios with increasing metamorphic grade until anatectic conditions are reached. In this way, granitic melts derived from a source at depth do not necessarily have to match the isotopic composition of the equivalent metamorphic rocks at the level of granite emplacement. The available data for acid–intermediate meta-igneous lower crustal rocks in several orogenic segments seem to indicate a shift in Sr–Nd compositions towards bulk earth values when compared to the same metamorphic rocks in upper crustal levels (e.g., French Massif Central, compare data for the meta-igneous lower crustal rocks of Downes and Duthou, 1988 with the data for the outcropping meta-igneous rocks of Turpin et al., 1990). Granulite facies lower crustal orthogneisses tend to decrease their Sr isotopic ratios more markedly than their Nd isotopic ratios which are much less modified (Fig. 11a). This displacement of the isotopic composition seems to be present in different types of crustal rocks undergoing granulite facies metamorphism in the lower crust (e.g., Ruiz et al., 1988), and it may explain the whole range of Sr–Nd compositions observed in the SCR plutons.

Another process which may be imposed on the aforementioned progressive isotopic change with increasing metamorphic grade is isotopic disequilibrium during partial melting. In high grade anatectic areas, incomplete isotopic resetting during migmatite formation has been observed. In a study of the Hercynian granitoids of the Anatectic Complex of
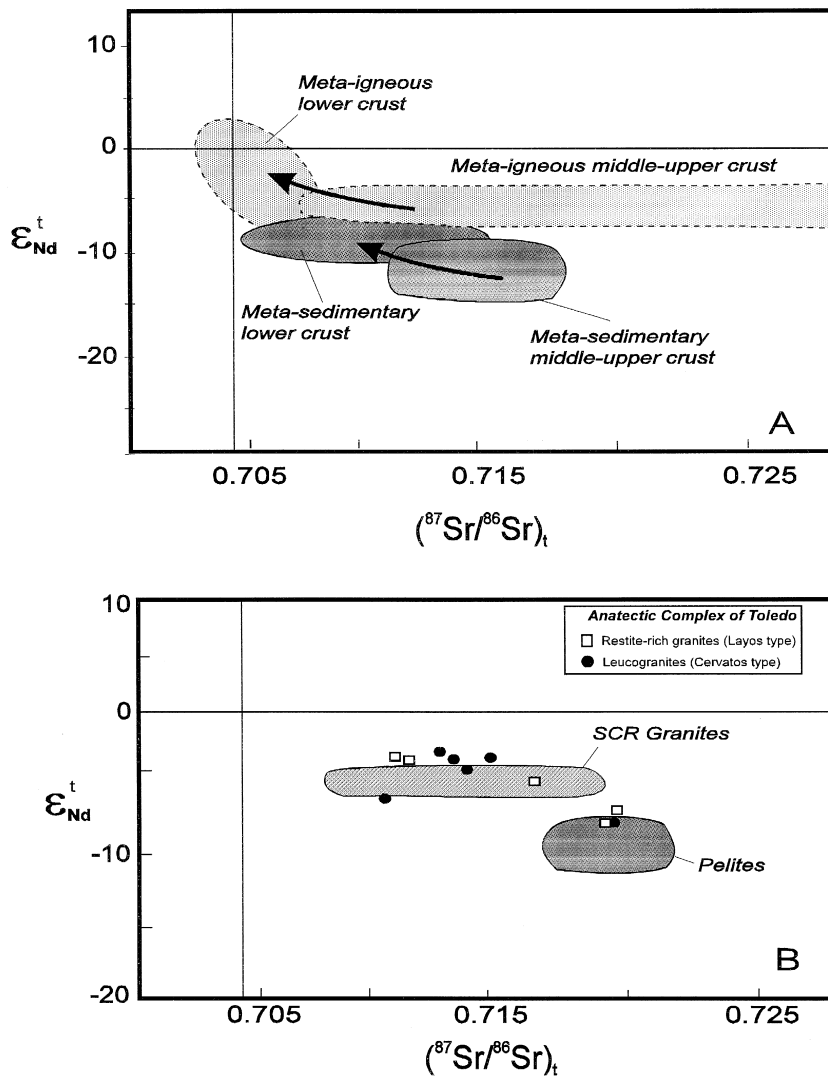
Fig. 11. (a) Initial $^{87}Sr/^{86}Sr$ vs. initial ε_{Nd} plot showing the fields of meta-igneous and meta-sedimentary middle-upper crust and meta-igneous and metasedimentary lower crustal xenoliths from the French Massif Central (Turpin et al., 1990; Downes and Duthou, 1988). (b) Initial $^{87}Sr/^{86}Sr$ vs. initial ε_{Nd} plot from granites and metapelitic rocks from the Anatectic Complex of Toledo, ACT (Barbero et al., 1995). In this figure, the compositional field for the epizonal peraluminous granites of this study is also displayed. Initial ratios for the ACT rock were calculated assuming an age of 340 Ma. The ACT catazonal peraluminous granites are interpreted as isotopically disequilibrated melts from pelitic protoliths (Barbero et al., 1995). Notice the lowering in Sr and Nd initial ratios of the anatectic leucogranites compared to their pelitic protoliths, and their isotopic similarity to later epizonal granitoids.

Toledo, Barbero et al. (1995) showed that the pelite-derived anatectic leucogranites had higher initial ε_{Nd} and lower initial $^{87}Sr/^{86}Sr$ than the local granulite facies pelitic materials. These crustal-derived granitic rocks have the same isotopic composition as the epizonal peraluminous plutons of this study (Fig. 11b). Recent experimental results indicate that the

stoichiometry of the melting reaction, together with the kinetics of melting, are the main factors controlling the isotopic composition of the melts and not the bulk composition of the source rock (Hammouda et al., 1994). So, an enrichment in biotite and accessory minerals in the mesosomes compared to the leucosomes could explain the observed isotopic differ-

ences. If the possibility of having isotopic disequilibrium in migmatitic rocks is real, such a process must also be considered in higher melting rate scenarios.

6.4. Model ages

The SCR granites give T_{DM}^{Nd} model ages in the range 1.4 to 1.6 Ga, as is common in Hercynian granites (Liew and Hofmann, 1988; Pin and Duthou, 1990; Moreno-Ventas et al., 1995) (Fig. 12). The model ages are calculated with the Liew and Hofmann (1988) equation, which assumes an average pre-crystallization crustal Sm/Nd ratio of 0.12 in order to correct for any fractionation of Sm/Nd in the granitoids due to minor phase control during crystallization of the granites. The use of the actual Sm/Nd ratios results in the more felsic varieties giving anomalously old model ages (2.0 to 4.9 Ga).

The model ages for the granites are coincident with model T_{DM} ages in the orthogneisses, but not with those of the metasediments (Table 3 and Fig. 12). This 'regional equilibrium signature' shown by

the granites and surrounding country rocks is common in Hercynian areas (Liew and Hofmann, 1988; Bickle et al., 1988) and is also maintained in deep crustal xenoliths (Downes and Leyreloup, 1986). This is most simply interpreted as indicating that any juvenile crustal additions during the Phanerozoic have not drastically affected the average regional basement values.

6.5. Factors controlling the crustal generation of the SCR granites

There must be two main factors contributing to the generation of granitic magmatism in the SCR; firstly, the considerable crustal thickening which occurred during the Hercynian orogeny, and secondly, the relatively radiogenic character of the protoliths involved in the granite genesis. Villaseca and Barbero (1994b) estimated pressures and temperatures for the maximum tectonic thickening in the range 14 ± 1 kb and $700 \pm 50°C$ on the basis of the presence of residual omphacitic pyroxene included in
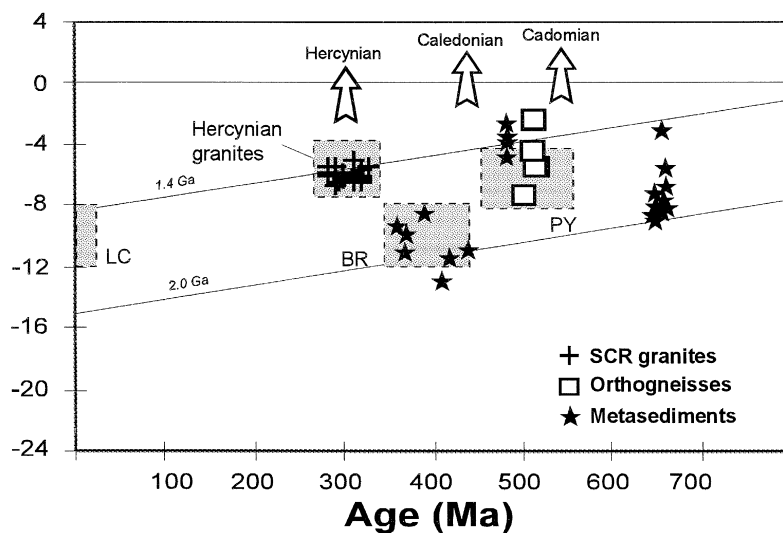

Fig. 12. Plot of initial ε_{Nd} vs. age displaying data from this study (crosses = Hercynian granites; squares = Cadomian orthogneisses; stars = pre-Ordovician metasedimentes and those of Nägler et al. (1995) for Paleozoic metasediments of Central Iberian Zone (CIZ, Spain); other data from Michard et al. (1985) (metasediments of Britanny, BR, and Pyrenees, PY), Downes and Leyreloup (1986) (metasedimentary xenoliths from lower crust from the Massif Central, LC), Liew and Hofmann (1988) (European Hercynian granites). We assume a Cadomian age for CIZ orthogneisses based on the Rb–Sr data from Vialette et al. (1987) and U–Pb data of zircons from Wildberg et al. (1989). A Proterozoic age of 650–665 Ma for the pre-Ordovician metasediments is adopted on the basis of stratigraphic criteria after López Díaz (1994). Reference T_{DM} age evolution lines for 1.4 and 2.0 Ga average continental crust were calculated assuming a typical crustal $^{147}Sm/^{144}Nd$ ratio of 0.12 using Liew and Hofmann (1988) formula.

pyrope-rich garnet in metabasites. These P–T conditions, together with the actual thickness of the continental crust in this area, led to an estimation of 75–80 km for the crustal thickness in Hercynian times, which is not unusual in the European Hercynides (Medaris et al., 1995). The fact that the acid magmatism persists for a time span of at least 50 Ma is satisfactorily explained in a thickened crust scenario in which several mid-lower crustal segments could reach melting conditions (England and Thompson, 1986; Patiño Douce et al., 1990).

The composition of the crust in the studied area is essentially sialic with only a minor basic component, and so, the radioactive heat generation is high. Considering the K, Th, and U contents of the crustal lithologies of the area (K is 1.7–1.8, Th is 3.2–3.7, and U is 2.7–2.9 times richer than the average crustal composition from Weaver and Tarney, 1984), the average heat production ratio in intermediate orthogneisses is 2.8 μW m^{-3}, and in metapelites (granulite facies terranes of low-pressure conditions) it is 3.1 μW m^{-3}, according to the formulation of Rybach (1976). These values are much higher than the typical values used in theoretical models of anatexis in tectonically thickened continental crust (England and Thompson, 1986; 0.86–1.29 μW m^{-3}). As England and Thompson (1986) stated, a 50% increase in internal radiogenic heat production raises peak temperatures by more than 150°C in the bottom half of the crust (keeping all other parameters constant). Heat production rate values in the SCR are even higher than those used by Patiño Douce et al. (1990) for the crustal model of the Sevier hinterland where these authors calculated temperatures of 900°C at the bottom of the crust without any perturbation in the basal heat flux. In those models, thickening of 1.5 to 2 times the original crustal thickness resulted in widespread anatexis at middle and lower crustal levels. It is important to remember that the crustal thickness in this area during the Hercynian might have been 2.5 times the pre-Hercynian thickness (Villaseca and Barbero, 1994b), and this might be enough to explain the P–T conditions achieved in the area. The scarce basic magmatism in the area may have enhanced the thermal budget of the crust, though, as documented earlier, this did not play a major role in controlling the chemical variability of the granitic series. Furthermore, geophysical work

performed in the area has not recognised any important basic layer in the Hercynian crust of Central Spain (Carbó and Capote, 1985), nor is there any evidence for the presence of high velocity layers over the Moho discontinuity (Iliha DSS Group, 1993). This, together with the almost complete absence of lower crustal basic granulitic xenoliths in Mesozoic dykes (Villaseca and Nuez, 1986), suggests that basaltic underplating of the lower crust was not important in this region during Hercynian times.

7. Conclusions

From the geochemical and isotopic data for the peraluminous granites, associated basic–intermediate rocks and metamorphic rocks a number of conclusions can be drawn.

(1) In the SCR, two peraluminous granitoid series with similar evolutionary geochemical trends can be distinguished. Crystal fractionation can explain the main major and trace element variability shown by the granitic plutons. The difference in accessory phases between both granite types leads to contrasting differentiation trends for certain trace elements such as Th, Nb, Y, and HREE in the more evolved magmas.

(2) Initial Sr and Nd isotope ratios in both peraluminous granitic series show the same range of values. Initial ε_{Nd} shows a narrow variation compared with that of the initial Sr ratios. This similarity of initial isotopic ratios and trace element geochemistry suggests similar sources for the PI and PS granites of the SCR. Differences in the degree of peraluminosity between the two series are probably controlled by different melting conditions.

(3) The associated basic and intermediate rocks, although following the geochemical trends of the granites for many elements, do not seem to have played a major role in controlling the chemical variability of the peraluminous granites, as previously reported. Geochemical modelling of the Sr–Nd isotopic composition of the granites using binary mixing between the basic material and crustal partial melts, and AFC processes involving the country rocks require an unrealistically high mantle contribution. Nevertheless, in some less felsic marginal fa-

cies of the granitic plutons, which are richer in mafic microgranular enclaves minor mixing between coeval basic and acidic magmas may have occurred.

(4) The isotopic compositions of the metamorphic country rocks do not match those of the peraluminous granites. Nevertheless, meta-igneous rocks (orthogneisses) better approach isotope signatures of the granites than metasedimentary country rocks. This is consistent with the results obtained by other authors for the origin of peraluminous Hercynian batholiths in western Europe (Downes and Duthou, 1988; Turpin et al., 1990).

(5) Based on the data presented, the possibility of disequilibrium partial melting of lower crustal sources and/or the lowering of the isotopic ratios during granulitization of the lower crust may better explain the isotopic data of the peraluminous granites than the involvement of an unsampled crustal protolith, as suggested in other peraluminous batholiths (Bernard-Griffiths et al., 1985; Clarke et al., 1988).

Acknowledgements

References

Andonaegui, P., 1990. Geoquímica y geocronología de los granitoides del sur de Toledo. PhD Thesis, Universidad Complutense de Madrid, p. 365.

Aparicio, A., Borschevski, Y.A., Borisova, S.L., Novitsky, Y., García Cacho, L., 1986. Relaciones isotópicas de $\delta^{18}O$ en el ambiente plutónico—metamórfico del Sistema Central Español (Sector Somosierra–Guadarrama). Bol. Geol. Min. España 97, 132–141.

Arth, J.G., 1976. Behaviour of trace elements during magmatic processes. A summary of theoretical models and their applications. J. Res. US Geol. Surv. 4, 41–67.

Barbero, L., 1995. Granulite facies metamorphism in the Anatectic Complex of Toledo (Spain): late-Hercynian tectonic evolution by crustal extension. J. Geol. Soc. London 152, 365–382.

Barbero, L., Villaseca, C., 1992. The Layos Granite, Hercynian Complex of Toledo (Spain): an example of parautochthonous restite-rich granite in a granulitic area. Trans. R. Soc. Edinburgh: Earth Sci. 83, 127–138.

Barbero, L., Villaseca, C., Rogers, G., Brown, P.E., 1995. Geochemical and isotopic disequilibrium in crustal melting: an insight from the anatectic granitoids from Toledo, Spain. J. Geophys. Res. 100 (B8), 15745–15765.

Bea, F., Fershtater, G., Corretge, L.G., 1992. The geochemistry of phosphorous in granite rocks and the effect of aluminium. Lithos 29, 43–56.

Bernard-Griffiths, J., Peucat, J.J., Sheppard, S., Vidal, P., 1985. Petrogenesis of Hercynian leucogranites from the southern Armorican Massif: contribution of REE and isotopic (Sr, Nd, Pb and O) geochemical data to the study of source rocks characteristics and age. Earth Planet. Sci. Lett. 74, 235–250.

Bickle, M.J., Wickham, S.M., Chapman, H.J., Taylor, H.P. Jr., 1988. A strontium, neodymium and oxygen isotope study of hydrothermal metamorphism and crustal anatexis in the Trois Seigneurs Massif, Pyrenees, France. Contrib. Mineral. Petrol. 100, 399–417.

Brandebourger, E., 1984. Les granitoides Hercyniens tardifs de la Sierra de Guadarrama (Système Central Espagne). Pétrographie et geochimie. PhD Thesis, Universite Lorraine, p. 209.

Carbó, A., Capote, R., 1985. Estructura actual de la corteza en el Sistema Central Español e implicaciones geotectónicas. Rev. Real Acad. C. Exactas, Físicas y Naturales 79, 625–634.

Casillas, R., 1989. Las asociaciones plutónicas tardihercínicas del sector occidental de la Sierra de Guadarrama, Sistema Central Español, (Las Navas del Marqués–San Martín de Valdeiglesias). Petrología, Geoquímica, Génesis y Evolución. PhD Thesis, Universidad Complutense de Madrid, p. 316.

Casillas, R., Vialette, Y., Peinado, M., Duthou, J.L., Pin, C., 1991. Ages et caracteristiques isotopiques (Sr–Nd) des granitoides de la Sierra de Guadarrama occidentale (Espagne). Abstract Séance specialissé de la Soc Geol France à la memoire de Jean Lameyre.

Champion, D.C., Chappell, B.W., 1992. Petrogenesis of felsic I-type granites: an example from northern Queensland. Trans. R. Soc. Edinburgh: Earth Sci. 83, 115–126.

Christiansen, J.N., DePaolo, D.J., 1993. Time scales of large volume silicic magma systems: Sr isotope systematics of phenocrysts and glass from the Bishop Tuff, Long Valley, California. Contrib. Mineral. Petrol. 113, 100–114.

Clarke, D.B., Halliday, A.N., Hamilton, P.J., 1988. Neodymium and strontium isotopic constraints on the origin of the peraluminous granitoids of the South Mountain Batholith, Nova Scotia. Chem. Geol. 73, 15–24.

Cocherie, A., Rossi, P., Fouillac, A.M., Vidal, P., 1994. Crust and

mantle contribution to granite genesis. An example from the Variscan batholith of Corsica, France, studied by trace-element and Nd–Sr–O-isotope systematics. Chem. Geol. 115, 173–211.

Conrad, W.K., Nicholls, I.A., Wall, V.J., 1988. Water-saturated and undersaturated melting of metaluminous and peraluminous crustal composition at 10 kb: evidence for the origin of silicic magmas in the Taupo Volcanic Zone, New Zealand, and other occurrences. J. Petrol. 29, 765–803.

Debon, F., Le Fort, P., 1983. A chemical–mineralogical classification of common plutonic rocks and associations. Trans. R. Soc. Edinburgh: Earth Sci. 73, 135–149.

DePaolo, D.J., 1981. Trace element and isotopic effects of combined wallrock assimilation and fractional crystallization. Earth Plant. Sci. Lett. 53, 189–202.

Dias, G., Leterrier, J., 1994. The genesis of felsic–mafic plutonic associations: a Sr and Nd isotopic study of the Hercynian Braga Granitoids Massif (Northern Portugal). Lithos 32, 207–223.

Di Vincenzo, G., Andriessen, P.A.M., Ghezzo, C., 1996. Evidence of two different components in a Hercynian peraluminous cordierite-bearing granite: the San Basilio intrusion (Central Sardinia, Italy). J. Petrol. 37, 1175–1206.

Doblas, M., 1991. Late-Hercynian extensional and transcurrent tectonics in central Iberia. Tectonophysics 191, 325–334.

Downes, H., Leyreloup, A., 1986. Granulite xenoliths from the French Massif Central—petrology, Sr and Nd isotope systematics and model age estimates. In: Dawnes, J.B., Carswell, D.A., Hall, J., Wedepohl, K.H. (Eds.), Nature of the Lower Continental Crust. Geol. Soc. Special Publ., Vol. 24, pp. 319–330.

Downes, H., Duthou, J.L., 1988. Isotopic and trace element arguments for the lower-crustal origin of Hercynian granitoids and pre-Hercynian orthogneisses, Massif Central (France). Chem. Geol. 68, 291–308.

England, P.C., Thompson, A.B., 1986. Some thermal and tectonic models for crustal melting in continental collision zones. In: Coward, M.P., Ries, A. (Eds.), Collision Tectonics. Geol. Soc. Spec. Publ., Vol. 19, pp. 83–94.

Förster, H.J., Tischendorf, G., 1994. Evolution of the Hercynian granite magmatism in the Erzgebirge metallogenic province. Min. Mag. A 58, 284–285.

Fúster, J.M., Rubio, J.I., 1980. El afloramiento granodiorítico–tonalítico de La Ventosilla (Guadarrama Central). Bol. Geol. Min. 91, 494–502.

Govindaraju, K., Mevelle, G., 1987. Fully automated dissolution and separation methods for inductively coupled plasma atomic emission spectrometry rock analysis—application to the determination of rare earth elements. J. Anal. Atom. Spectrom. 2, 615–621.

Hammouda, T., Pichavant, M., Chaussidon, M., 1994. Mechanism of isotopic equilibration during partial melting: an experimental test of the behaviour of Sr. Min. Mag. A 58, 368–369.

Holtz, F., Johannes, W., 1991. Genesis of peraluminous granites: I. Experimental investigation of melt composition at 3 and 5 kb and various H_2O activities. J. Petrol. 32, 909–934.

Ibarrola, E., Villaseca, C., Vialette, Y., Fúster, J.M., Navidad, M.,

Peinado, M., Casquet, C., 1987. Dating of Hercynian granites in the Sierra de Guadarrama (Spanish Central System). In: Bea, F., Carnicero, A., Gonzalo, J.C., López-Plaza, M., Rodríguez-Alonso, M.D. (Eds.), Geología de los granitoides y rocas asociadas del Macizo Hespérico. Rueda, Madrid, pp. 377–383.

Iliha DSS Group, 1993. A deep seismic sounding investigation of lithospheric heterogeneity and anisotropy beneath the Iberian Peninsula. Tectonophysics 221, 35–51.

Janousek, V., Rogers, G., Bowes, D.R., 1995. Sr–Nd isotopic constraints on the petrogenesis of the Central Bohemian Pluton, Czech Republic. Geol. Rundsch. 84, 520–534.

Kwan, T.S., Krähenbül, R., Jäger, E., 1992. Rb–Sr, K–Ar and fission track ages for granites from Penang Island, West Malaysia: an interpretation model for Rb–Sr whole rock and for actual experimental mica data. Contrib. Mineral. Petrol. 111, 527–542.

Lallena, P.P., Sanz, H.G., Pérez del Villar, L., Quejido, A.J., 1990. Datación absoluta de granitoides de la Sierra de Gredos, por el método Rb–Sr. Bol. Soc. España Min. 13, 144–145.

Le Fort, P., Cuney, M., Deniel, C., France-Lanord, C., Sheppard, S.M.F., Upreti, B.N., Vidal, P., 1987. Crustal generation of the Himalayan leucogranites. Tectonophysics 134, 39–57.

Liew, T.C., Hofmann, A.W., 1988. Precambrian crustal components, plutonic associations, plate environment of the Hercynian Fold Belt of Central Europe: indications from a Nd and Sr study. Contrib. Mineral. Petrol. 98, 129–138.

Liew, T.C., Finger, F., Höck, V., 1989. The Moldanubian granitoid plutons of Austria: chemical and isotopic studies bearing on their environmental setting. Chem. Geol. 76, 41–55.

López Díaz, F., 1994. Estratigrafía de los materiales anteordovícicos del anticlinal de Navaelpino (Zona Centroibérica). Rev. Soc. Geol. España 7, 31–45.

Masuda, A., Nakamura, N., Tanaka, T., 1973. Fine structures of mutually normalised rare earth patterns of chondrites. Geochim. Cosmochim. Acta 37, 239–248.

McCulloch, M.T., Chappell, B.W., 1982. Nd isotopic characteristics of S- and I-type granites. Earth Planet. Sci. Lett. 58, 51–64.

Medaris, L.G., Beard, B.L., Johnson, C.M., Valley, J.W., Spicuzza, M.J., Jelinek, E., Mísâr, Z., 1995. Garnet pyroxenite and eclogite in the Bohemian Massif: geochemical evidence for Variscan recycling of subducted lithosphere. Geol. Rundsch. 84, 481–505.

Michard, A., Gurriet, P., Soudant, M., Albarède, F., 1985. Nd isotopes in French Phanerozoic shales: external vs. internal aspects of crustal evolution. Geochim. Cosmochim. Acta. 49, 601–610.

Miller, C.F., 1985. Are strongly peraluminous magmas derived from pelitic sedimentary sources?. J. Geol. 93, 673–689.

Moreno-Ventas, I., Rogers, G., Castro, A., 1995. The role of hybridization in the genesis of Hercynian granitoids in the Gredos Massif, Spain: inferences from Sr–Nd isotopes. Contrib. Mineral. Petrol. 120, 137–149.

Nägler, T.F., Schäfer, H.J., Gebauer, D., 1995. Evolution of the Western European continental crust: implication from Nd and Pb isotopes in Iberian sediments. Chem. Geol. 121, 345–357.

Nash, W.P., Crecraft, H.R., 1985. Partition coefficients for trace elements in silicic magmas. Geochim. Cosmochim. Acta 49, 2309–2322.

Patiño Douce, A.E., 1994. Melt generation in the continental crust: answered and unanswered questions. Min. Mag. A 58, 692–693.

Patiño Douce, A.E., Johnston, A.D., 1991. Phase equilibria and melt productivity in the pelitic system: implications for the origin of peraluminous granitoids and aluminous granulites. Contrib. Mineral. Petrol. 107, 202–218.

Patiño Douce, A.E., Humphreys, D.E., Johnston, A.D., 1990. Anatexis and metamorphism in tectonically thickened crust exemplified by the Sevier Hinterland, Western North America. Earth Planet. Sci. Lett. 97, 290–315.

Pérez-Soba, C., 1991. Petrología y geoquímica del macizo granítico de La Pedriza. PhD Thesis, Universidad Complutense de Madrid, 225 pp.

Pin, C., Duthou, J.L., 1990. Sources of Hercynian granitoids from the French Massif Central: inferences from Nd-isotopes and consequences for crustal evolution. Chem. Geol. 83, 281–296.

Pinarelli, L., Rottura, A., 1995. Sr and Nd isotopic study and Rb–Sr geochronology of the Bejar granites, Iberian Massif, Spain. Eur. J. Mineral. 7, 577–589.

Pitcher, W.S., 1978. The anatomy of a batholith. J. Geol. Soc. London 135, 157–182.

Poli, G., Tommasini, S., Halliday, A.N., 1996. Trace element and isotopic exchange during acid–basic magma interaction processes. Trans. R. Soc. Edinburgh: Earth Sci. 87, 225–232.

Rogers, G., Hawkesworth, C.J., 1989. A geochemical traverse across the North Chilean Andes: evidence for crust generation from the mantle wedge. Earth Planet. Sci. Lett. 91, 271–285.

Rollinson, H., 1993. Using geochemical data: evaluation, presentation, interpretation. Longman, Essex, pp. 352.

Ruiz, J., Patchett, P.J., Arculus, R.J., 1988. Nd–Sr isotopic composition of lower crustal xenoliths—evidence for the origin of mid-Tertiary felsic volcanics in Mexico. Contrib. Mineral. Petrol. 99, 36–43.

Rybach, L., 1976. Radioactive heat production: a physical property determined by the chemistry of rocks. In: Strens, R.G.J. (Ed.), The Physics and Chemistry of Minerals and Rocks. Wiley, London, pp. 309–318.

Sparks, R.S.J., Marshall, L.A., 1986. Thermal and mechanical constraints on mixing between mafic and silicic magmas. J. Volc. Geoth. Res. 29, 99–124.

Shaw, A., Downes, H., Thirlwall, M.F., 1993. The quartz–diorites of Limousin: elemental and isotopic evidence for Devono-Carboniferous subduction in the Hercynian belt of the French Massif Central. Chem. Geol. 107, 1–18.

Stephens, W.E., Holden, P., Henney, P.J., 1991. Microdioritic enclaves in the Scottish Caledonian granitoids and their significance for crustal magmatism. In: Didier, J., Barbarin, B. (Eds.), Enclaves and granite petrology. Elsevier, Amsterdam, pp. 125–134.

Thompson, R.N., Morrison, M.A., Hendry, G.L., Parry, S.J., 1984. An assessment of the relative roles of crust and mantle magma genesis: an elemental approach. Philos. Trans. R. Soc. London A 310, 549–590.

Turpin, L., Cuney, M., Friedrich, M., Bouchez, J.L., Aubertin, M., 1990. Meta-igneous origin of Hercynian peraluminous granites in the NW French Massif Central: implications for crustal history reconstructions. Contrib. Mineral. Petrol. 118, 13–32.

Valverde-Vaquero, P., Hernaiz, P.P., Escuder, J., Dunning, G.R., 1995. Comparison of the pre-Cambrian and Palaeozoic evolution of the Sierra de Guadarrama (Central Iberian Zone, Spain) and the Gondwana margin, NFLD Appalachians (GMNA). Terra Abstr. 7, 278.

Vialette, Y., Bellido, F., Fúster, J.M., Ibarrola, E., 1981. Données géochronologiques sur les granites de la Cabrera. Cuad. Geol. Ibérica 7, 327–335.

Vialette, Y., Casquet, C., Fuster, J.M., Ibarrola, E., Navidad, M., Peinado, M., Villaseca, C., 1987. Geochronological study of orthogneisses from the Sierra de Guadarrama (Spanish Central System). Neues Jb. Miner. Mh. Jq. H 10, 465–479.

Vielzeuf, D., Holloway, J.R., 1988. Experimental determination of the fluid-absent melting relations in the pelitic system. Consequences for crustal differentiation. Contrib. Mineral. Petrol. 98, 257–276.

Villaseca, C., Nuez, J., 1986. Diques camptoníticos en el Sistema Central Español. Est. Geol. 42, 69–77.

Villaseca, C., Barbero, L., 1994a. Chemical variability of Al–Fe–Ti–Mg minerals in peraluminous granitoid rocks from Central Spain. Eur. J. Mineral. 6, 691–710.

Villaseca, C., Barbero, L., 1994b. Estimación de las condiciones del metamorfismo hercínico de alta presión de la Sierra de Guadarrama. Geogaceta 16, 27–30.

Villaseca, C., Barbero, L., Huertas, M.J., Andonaegui, P., Bellido, F., 1993. A cross-section through Hercynian granites of Central Iberian Zone. Excursion guide. C.S.I.C., Madrid, 122 pp.

Villaseca, C., Eugercios, L., Snelling, N.J., Huertas, M.J., Castellón, T., 1995. Nuevos datos geocronológicos (Rb–Sr, K–Ar) de granitoides hercínicos de la Sierra de Guadarrama. Rev. Soc. Geol. España 8, 129–140.

Weaver, B., Tarney, J., 1984. Empirical approach to estimating the composition of the continental crust. Nature 310, 575–577.

White, A.J.R., Chappell, B.W., 1989. Geology of the Numbla 1:100,000 Sheet (8624). Geol. Surv. NSW, Sydney.

Wildberg, H.G.H., Bischoff, L., Baumann, A., 1989. U–Pb ages of zircons from meta-igneous and metasedimentary rocks of the Sierra de Guadarrama: implications for the Central Iberian crustal evolution. Contrib. Mineral. Petrol. 103, 253–262.

Williamson, J.H., 1968. Least squares fitting of a straight line. Can. J. Phys. 46, 1845–1847.